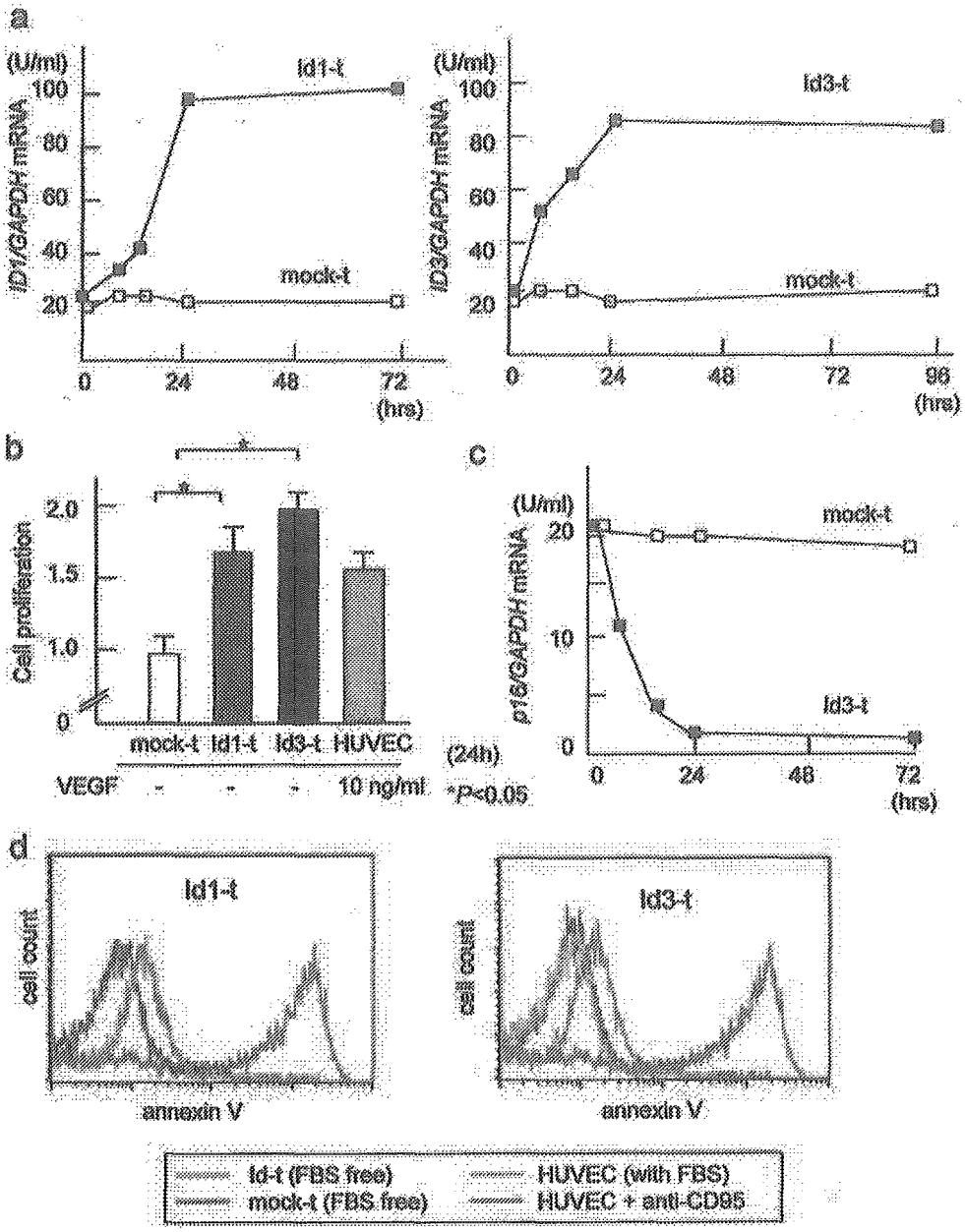

FIGURE 2. Overexpression of *ID1* or *ID3* induces proliferation of HUVECs. *a*, pBLAST49-hId1a(c) (Id1-t), pBLAST49-hId3(c) (Id3-t), or pBLAST49-mcs (mock-t) vector was transfected into HUVECs. Total RNA was isolated from each transfectant, and Id1 or Id3 mRNA level was sequentially quantitated using real-time RT-PCR. *b*, Proliferation of HUVECs at 24 h after transfection. Id1-t and Id3-t exhibited significantly higher proliferation in the absence of VEGF, compared with mock transfectants. Proliferation of Id transfectants was comparable with that of untransfected HUVECs stimulated with 10 ng/ml VEGF. Proliferation was measured using WST-1 assay. *c*, $p16^{INK4a}$ mRNA levels of *ID3* and mock transfectants were measured with real-time RT-PCR. $p16^{INK4a}$ mRNA expression was inversely correlated with Id3 mRNA shown in *a*. *d*, Apoptosis was induced in Id1, Id3, or mock transfectants by serum deprivation for 48 h, and the cells were stained with Annexin V-FITC. Freshly split HUVECs with or without treatment with agonistic anti-Fas/CD95 Ab (7C11) were used as positive and negative controls, respectively. Apoptosis induction was inhibited by overexpression of Id3, but not by Id1.

Flow cytometry

HUVECs were harvested by washing with 0.02% EDTA-PBS followed by treatment with trypsin-EDTA (InvivoGen), resuspended in PBS containing 0.1% BSA (Sigma-Aldrich) and 0.1% sodium azide, and incubated for 30 min with 50 ng/ml human γ-globulin (Sigma-Aldrich) at room temperature, to block for nonspecific binding.

For direct immunofluorescence staining, the cells were incubated with fluorescence-labeled mAbs or the isotype-matched controls for 30 min on ice, and then washed three times using a washing buffer consisting of PBS containing 0.2% BSA and 0.1% sodium azide. For indirect immunofluorescence staining, the cells were incubated with unlabeled primary mAbs or the isotype-matched Abs for 30 min on ice, washed with washing buffer, and then incubated with PE-conjugated goat anti-mouse IgG (Beckman Coulter), followed by another washing in washing buffer. Fluorescence intensity was analyzed in the EPICS XL (Beckman Coulter) or in the FACSCalibur (BD Biosciences).

Transmigration assay

Transmigration assays were performed using 8-μm-pore Transwell chambers (Corning, Corning, NY). HUVECs harvested by trypsinization were resuspended in MCDB151 medium containing 0.2% BSA, and seeded at 1×10^4 cells per well on the gelatin-coated upper chambers. Lower chambers were filled with 600 μl of the same medium supplemented with 10% FBS without or with either VEGF (20 ng/ml) or IL-1β (0.5 ng/ml). After incubation for 8 h at 37°C, 60 μl of 0.2% EDTA-PBS was added to the lower wells, and cells were harvested. The number of cells in the region corresponding to endothelial cells was counted in the EPICS, after acquiring cells in each sample for 50 s. The assays were done in triplicate.

Zymography

HUVECs were seeded on uncoated 100-mm dishes at 1×10^6 cells/well and were incubated with a 1:1 mixture of serum-free DMEM and F-12 Ham's medium (Sigma-Aldrich) for 12 h at 37°C. Then, supernatants were collected and, after removal of cells by centrifugation, were concentrated using the Centricon YM-10 concentrator (Millipore, Bedford, MA). Samples were then diluted with the same volume of sample buffer, and the MMPs were separated in SDS-PAGE using 10% polyacrylamide gels containing 0.1% gelatin. The gels were then incubated in 6.25% Triton X-100 (Wako Pure Chemical) for 1 h to remove SDS, and then placed for overnight in an incubation buffer containing 5 mM $CaCl_2$ and 1 μM $ZnCl_2$ for development of enzyme activity. The gels were stained using Coomassie brilliant blue and destained in methanol/acetic acid. Gelatinase activity was detected as unstained bands.

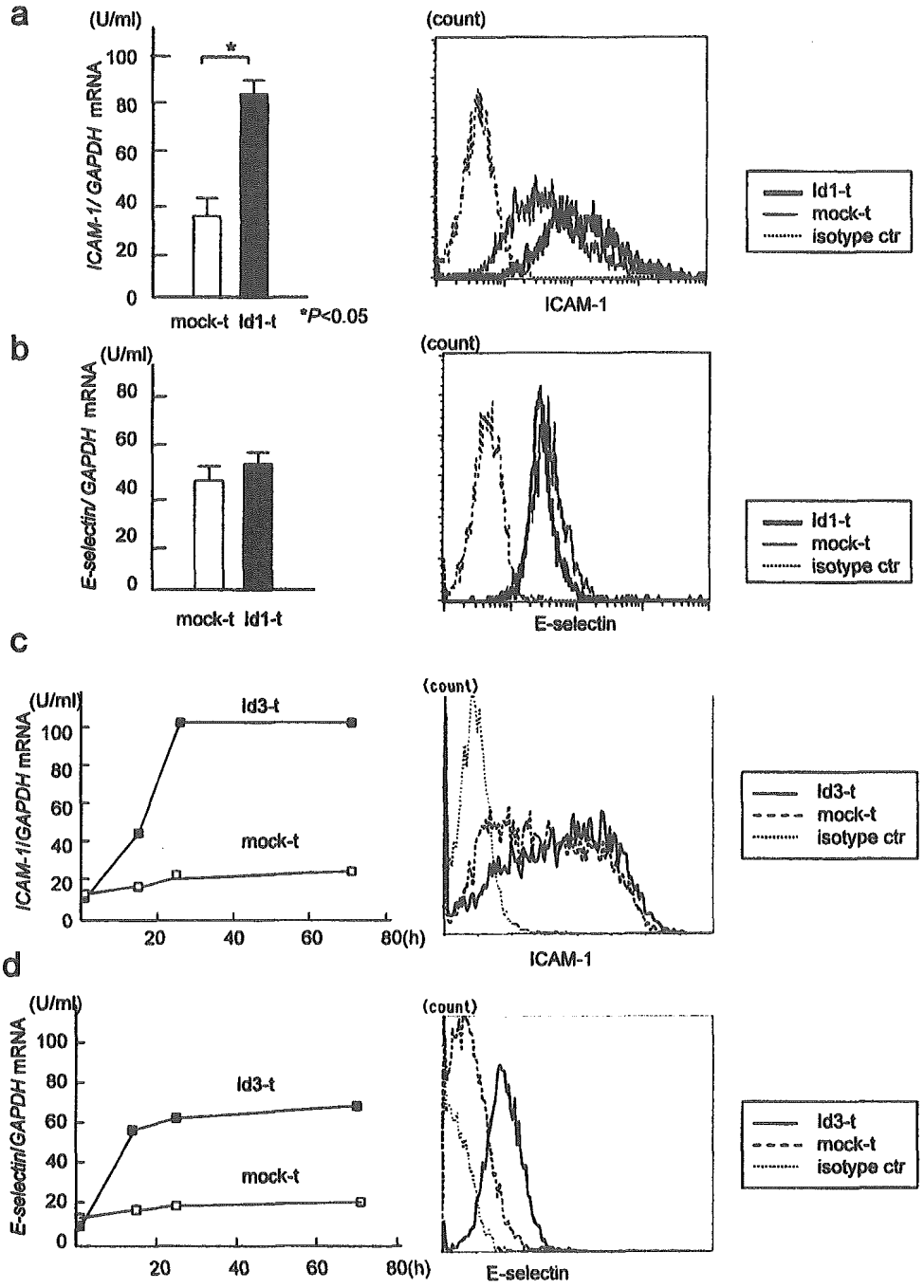

FIGURE 3. Overexpression of Id1 or Id3 induces activation of HUVECs. *a* and *b*, mRNA levels and surface expression of ICAM-1 (*a*) and E-selectin (*b*) in Id1 transfectants at 24 h after transfection. *c* and *d*, Kinetics of ICAM-1 (*c*) and E-selectin (*d*) mRNA levels in Id3 transfectants (*left*) and surface expression at 24 h. Significant up-regulation of ICAM-1 was observed in both transfectants, whereas expression of E-selectin was up-regulated only in Id3 transfectants.

In vitro tube formation

In vitro tube formation assay was performed using the Matrigel basement membrane matrix (BD Biosciences). Matrigel, kept on ice, was placed at 1 ml/well in six-well culture plates. The plates were then incubated at 37°C for 30 min to allow Matrigel to solidify. HUVECs were seeded at 5×10^4 cells per well on the top of the solidified Matrigel in the presence or absence of VEGF, and the plate was incubated at 37°C for 24 h. Tube formation on Matrigel was observed and analyzed under the microscope. The degree of angiogenesis was measured by multiplying the number of branch points by the total number of branches (23).

Statistics

Statistical significance was analyzed with Student's unpaired *t* test using StatView for Windows, version 5.0 (SAS Institute, Cary, NC).

Results

Induction of Id expression by VEGF and TGFβ in HUVECs

To gain insight into the significance of Id in relation to physiological endothelial cell activation and angiogenesis, we examined whether mRNA expression of Id1 and Id3 could be induced by known stimulators of endothelial cells such as VEGF, TGFβ, TNF-α, IL-1β, and bFGF. Significant up-regulation was observed for Id1 and Id3 mRNA when stimulated with VEGF (20 ng/ml) or TGFβ (0.5 ng/ml) (Fig. 1*a*). In contrast, expression of Id was not induced by IL-1β, TNF-α, or bFGF (Fig. 1, *b* and *c*).

Induction of proliferation of HUVECs by overexpression of Id

Next, we asked whether overexpression of Id alone could induce activation and proliferation of HUVECs. To address this question,

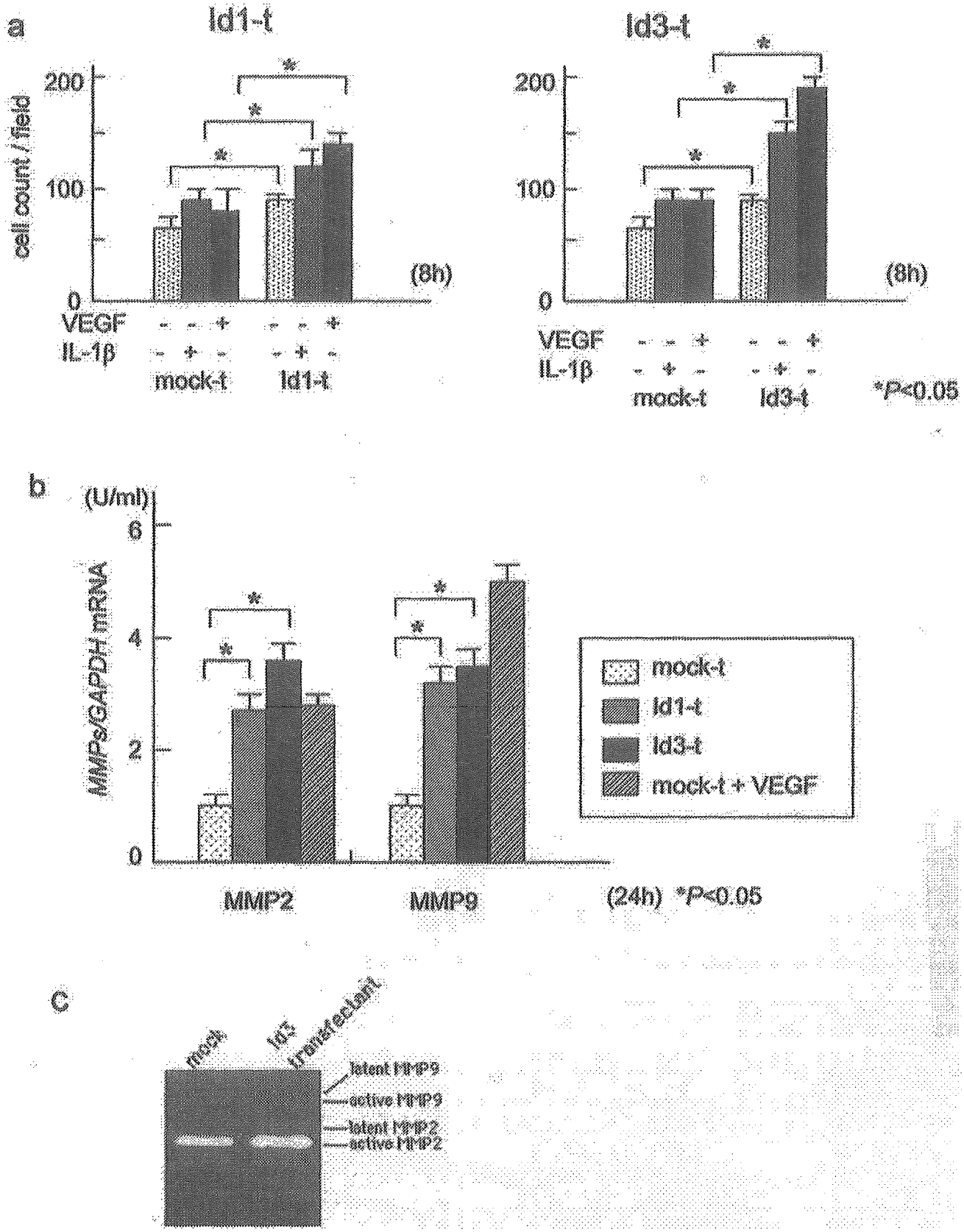

FIGURE 4. Overexpression of Id1 or Id3 induces angiogenic properties in HUVECs. *a*, Transmigration assay. Id1-t and Id3-t demonstrated significant increase in the transmigration activity, especially when the cells were stimulated with IL-1β (0.5 ng/ml) or VEGF (20 ng/ml). *b*, mRNA levels of MMP2 and MMP9. MMP2 and MMP9 expression was significantly increased in Id1-t and Id3-t. *c*, Zymography. Up-regulation of MMP2 and MMP9 activity was confirmed at the protein level.

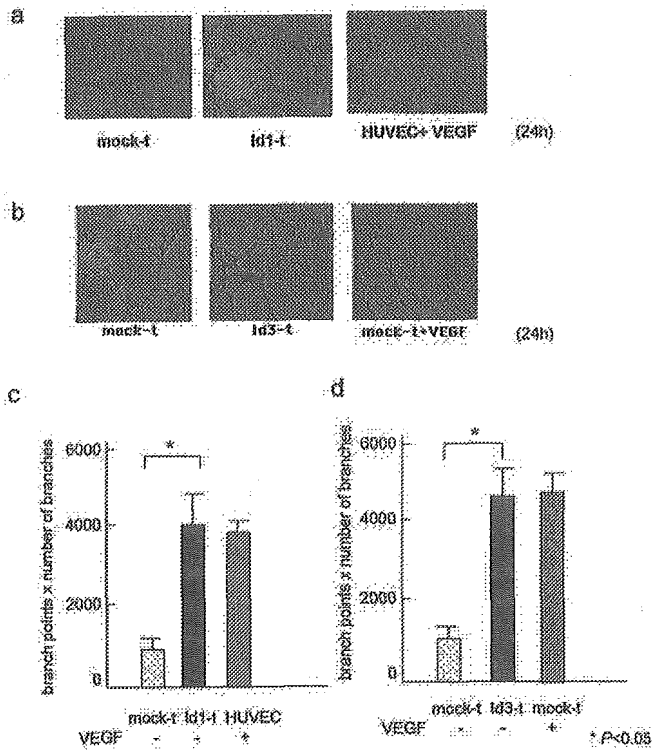

FIGURE 5. Enhanced tube formation by overexpression of Id1 or Id3 in the Matrigel. *a* and *b*, Id1-t (*a*) and Id3-t (*b*) exhibited enhanced tube formation in the Matrigel in the absence of VEGF (original magnification, ×100). *c* and *d*, The degree of tube formation in the transfectants at the basal level was comparable with mock transfectants cultured in the presence of VEGF (10 ng/ml).

transient overexpression of Id1 or Id3 was induced in HUVECs by transfection (Fig. 2*a*). Proliferation was significantly enhanced in both transfectants as compared with mock transfectant, to levels similar to the proliferative activity of untransfected HUVECs when stimulated with VEGF (Fig. 2*b*).

Id has been shown to regulate the cell cycle via transcriptional regulation of $p16^{INK4a}$ (16). In Id transfectants, the $p16^{INK4a}$ expression was found to be inversely correlated with expression level of *ID* mRNA (Fig. 2, *a* and *c*).

Id has also been shown to regulate apoptosis either positively or negatively, depending on the cell types (24, 25). The effect of Id overexpression on apoptosis was examined by serum starvation-induced apoptosis model. After the cells were cultured for 48 h without FBS, Id1 and mock transfectants exhibited comparable enhancement of annexin V binding compared with freshly split HUVEC. In contrast, annexin V binding was significantly inhibited in Id3 transfectants, suggesting that overexpression of Id3, but not Id1, inhibits HUVEC apoptosis induced by serum starvation (Fig. 2*d*).

Induction of activation markers in HUVECs by overexpression of Id

To examine whether Id overexpression alone can induce activation of HUVECs, we measured the expression levels of ICAM-1 (CD54) and E-selectin (CD62E) after transfection of Id1 or Id3 in the absence of VEGF. mRNA levels of ICAM-1 was significantly increased both in Id1 and Id3 transfectants (Fig. 3, *a* and *c*). Correspondingly, the cell surface expression of ICAM-1 was significantly up-regulated in Id1 transfectants (Fig. 3*a*) and, to a lesser extent, in Id3 transfectants (*c*). In contrast, mRNA level and surface expression of E-selectin was clearly up-regulated in Id3 transfectants (Fig. 3*d*) but not in Id1 transfectants (*b*). These results suggested that both Id1 and Id3 can induce activation of HUVEC, but their downstream pathways may not be identical.

Induction of angiogenic processes by overexpression of Id

We next examined whether overexpression of Id in HUVECs can induce angiogenesis. Both Id1 and Id3 transfectants exhibited significant increase in the transmigration activity, especially when the cells were cultured with IL-1β (0.5 ng/ml) or VEGF (20 ng/ml) (Fig. 4*a*).

MMP2 and MMP9 are MMPs relevant to angiogenic processes. Basal expression levels of MMP2 and MMP9 mRNA were significantly increased both in Id1 and Id3 transfectants, and were comparable to those of VEGF-stimulated mock transfectants (Fig. 4*b*). Zymography confirmed up-regulation of MMP2 and MMP9 enzymatic activities (Fig. 4*c*). In the transfectants, not only the total MMP2 and MMP9 expression levels, but also expression levels of the active forms of MMP2 and MMP9 were increased compared with mock transfectants. Furthermore, tube formation in the Matrigel assay was markedly enhanced both in Id1 and Id3 transfectants even in the absence of VEGF (Fig. 5). Taken together, these observations indicate that overexpression of Id alone can induce angiogenic processes in HUVECs.

Inhibition of VEGF-induced proliferation and activation of HUVECs by ID1 *and* ID3 *shRNA*

In the next sets of experiments, we addressed the question whether Id proteins are essential for proliferation, activation, and angiogenic processes of HUVECs induced by VEGF. To inhibit expression of Id1 and Id3, we used RNA interference (RNAi). HUVECs were doubly transfected with RNA expression vectors containing *ID1* and *ID3* shRNA at 0.125, 0.5, or 1 ng/ml. A dose-dependent inhibition of VEGF-induced Id3 (Fig. 6*a*) and Id1 (data not shown) expression was observed. Subsequent studies were conducted using 1 ng/ml *ID1* and *ID3* shRNA transfectants.

Id1/Id3 double-knockdown transfectants exhibited significantly decreased proliferation when stimulated with VEGF (Fig. 6*b*). With respect to adhesion molecules, mock transfectants showed modest up-regulation of surface expression of ICAM-1 (Fig. 6*c*), E-selectin (*d*), and substantial up-regulation of α_v integrin (*e*), when stimulated with VEGF. In *ID1* and *ID3* shRNA transfectants, up-regulation of these molecules were completely inhibited (Fig. 6, *c–e*). When HUVECs were treated with either *ID1* or *ID3* shRNA, VEGF-induced ICAM-1 expression was inhibited, but induction of E-selectin and α_v integrin were not (data not shown).

We next tested whether Id1/Id3 knockdown also inhibits HUVEC activation by IL-1β and TNF-α. IL-1β modestly up-regulated ICAM-1 expression, which was not inhibited by knockdown of Id1 and Id3 (Fig. 6*f*). In contrast, TNF-α-induced up-regulation of E-selectin was inhibited by knockdown of Id1 and Id3 (Fig. 6*g*).

Inhibition of VEGF-induced angiogenesis by ID1 *and* ID3 *shRNA*

We next examined whether Id1/Id3 double knockdown can inhibit the VEGF-induced angiogenic processes of HUVECs. VEGF-induced transmigration activities were abolished in *ID1* and *ID3* shRNA transfectants (Fig. 7*a*). mRNA expression of MMP2, but not MMP9, was significantly decreased by Id1/Id3 knockdown, when HUVECs were cultured in the presence of VEGF (20 ng/ml) (Fig. 7*b*). VEGF-induced tube formation in Matrigel was markedly decreased in *ID1* and *ID3* shRNA transfected cells (Fig. 7, *c* and *d*). Such inhibition of the angiogenic processes was accompanied by a down-regulation of α_2 and β_1 integrins in *ID1* and *ID3* shRNA transfectants (Fig. 6, *h* and *i*). Thus, these results indicate

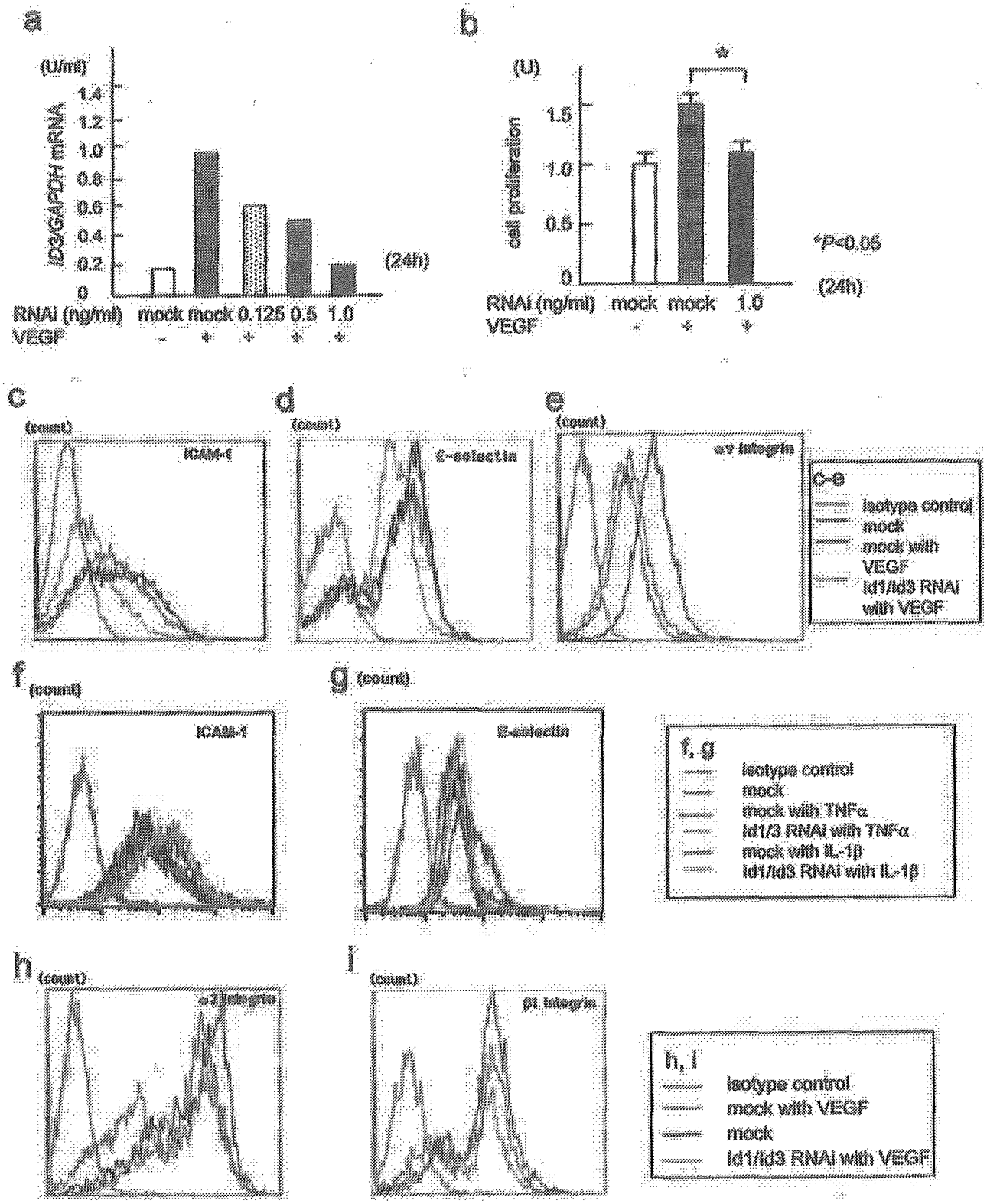

FIGURE 6. Silencing of Id1 and Id3 inhibits VEGF-induced proliferation and activation of HUVECs. *a*, HUVECs were transfected with *ID1* and *ID3* shRNA expression vectors at various concentrations or pSilencer alone (mock). After HUVECs were cultured for 24 h with or without VEGF (20 ng/ml), mRNA levels of *ID3* and *GAPDH* were quantitated. Dose-dependent suppression of *ID3* induction was observed. *ID1* induction was also inhibited (data not shown). *b*, Reduced VEGF-induced proliferation of double-knockdown transfectants. Proliferation was analyzed using WST-1 at 24 h. VEGF-induced proliferation was significantly inhibited in Id1/Id3 double-knockdown transfectants. *c–e*, Inhibition of VEGF-induced activation of HUVECs by Id1/Id3 double knockdown. Surface expression of ICAM-1 (*c*), E-selectin (*d*), and α_v integrin (*e*) was measured in mock transfectants with or without stimulation with VEGF (20 ng/ml), and *ID1* and *ID3* shRNA double transfectants stimulated with VEGF. Id1/Id3 double knockdown resulted in inhibition of VEGF-induced expression of ICAM-1, E-selectin, and α_v integrin. *f*, ICAM-1 expression was modestly up-regulated at 24 h after IL-1β treatment (1 ng/ml) in mock-t, which was not inhibited by knockdown of Id1/Id3. *g*, E-selectin expression was up-regulated at 5 h after TNF-α treatment (20 ng/ml) in mock-t, which was inhibited by silencing of Id1 and Id3. *h* and *i*, Surface expression of α_2 (*h*) and β_1 (*i*) integrins in *ID1*, *ID3* shRNA transfectants stimulated with VEGF (20 ng/ml). Both integrins were down-regulated.

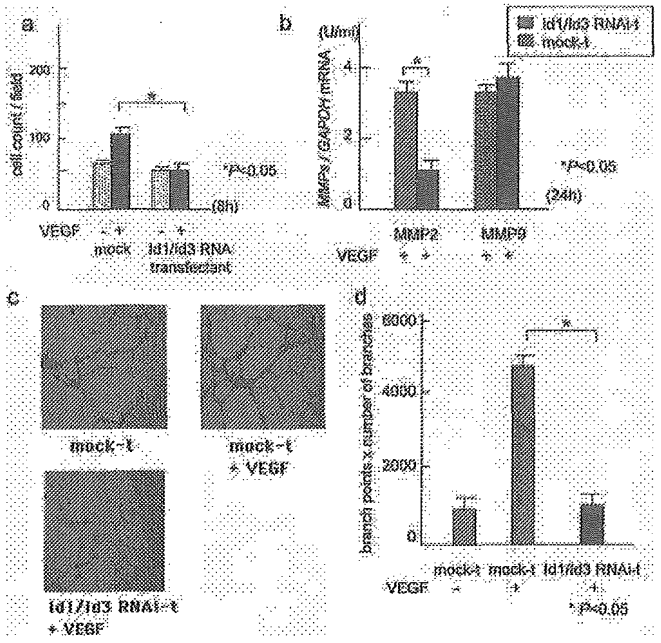

FIGURE 7. Silencing of Id1 and Id3 inhibits VEGF-induced angiogenic processes of HUVECs. *a*, Transmigration activity was significantly decreased in *ID1* and *ID3* shRNA transfectant after stimulation with VEGF (20 ng/ml) for 8 h. *b*, MMP mRNA expression in mock or *ID1* and *ID3* shRNA transfectants cultured for 8 h in the presence of VEGF (20 ng/ml). MMP2 mRNA expression was decreased in the double-knockdown cells, whereas MMP9 mRNA was not inhibited. *c*, Tube formation assay. Untransfected, mock-transfected, and *ID1*, *ID3* shRNA double-transfected HUVECs were cultured in the presence of VEGF (20 ng/ml) for 24 h. Marked inhibition of tube formation was observed by Id1/Id3 double knockdown. Original magnification, ×100. *d*, Quantitation of tube formation.

that the expression of Id plays a crucial role in the VEGF-induced angiogenic processes in HUVECs.

Discussion

In the present study, we demonstrated that overexpression of Id alone can induce proliferation, activation, and angiogenic processes of HUVECs in the absence of VEGF, to levels similar to that of VEGF-stimulated untransfected HUVECs. Moreover, knockdown of *ID1* and *ID3* in HUVECs almost completely abolished the VEGF-induced proliferation, activation, and angiogenic processes. These findings indicate a crucial role for Id in some of the VEGF signaling pathways in HUVECs.

Using $Id1^{+/-}Id3^{-/-}$ mice, it has been shown that Id expression is required to support angiogenesis in tumors (19), and that recruitment of $VEGFR1^{+}$ myeloid cells and $VEGFR2^{+}$ circulating endothelial precursor cells expressing Id is necessary for tumor growth (26). The new information presented in this study, including the requirement of Id also in human endothelial cells, up-regulation of ICAM-1 and E-selectin by forced expression of Id, and inhibition of endothelial cell activation and angiogenesis by double knockdown of Id1 and Id3, further emphasizes the crucial role of Id in endothelial cell activation and angiogenesis.

Previous reports demonstrated that Id controls the cell cycle in several ways (15), for example, by binding to Rb protein and blocking its tumor suppressor function (6, 12), or by inhibiting the binding of Ets1 and Ets2 transcription factors to $p16^{INK4a}$ promoter and repressing its expression (16). Our data suggested that at least the latter mechanism is operative in HUVECs. Id family proteins have been generally shown to promote apoptosis in a variety of conditions (24). However, in some settings, Id was shown to have antiapoptotic activity (25). Our present data suggested that overexpression of Id3, but not Id1, can protect HUVEC from apoptosis induced by serum starvation. In HUVECs, it was previously shown that VEGF prevents apoptosis induced by serum starvation (22). These results suggest that Id3 may mediate antiapoptotic effect induced by VEGF in HUVECs, and such an effect may also partly account for enhanced proliferation of Id3 transfectants.

As for ICAM-1 and E-selectin induction, it was recently demonstrated that VEGF induces these adhesion molecules in HUVECs through NF-κB (27), and that Id1 activates NF-κB transcription in prostate cancer cells (25). Our present data provide evidence that Id is involved in the signaling pathway that connects VEGF receptors and NF-κB activation in HUVECs. In our system, we have not distinguished contribution of each VEGFR for the induction of Id, which should be investigated in future studies. Although gene silencing of Id1 and Id3 efficiently inhibited ICAM-1 and E-selectin induction by VEGF and TNF-α, up-regulation of ICAM-1 by IL-1β was not inhibited. Taken together with the lack of *ID1* and *ID3* mRNA induction after stimulation with IL-1β, our results suggest that Id may not be involved in the IL-1β pathway of HUVEC activation. In the case of TNF-α stimulation, because mRNA of *ID* was not up-regulated, the presence of basal level of Id may be necessary for the activation of HUVEC by TNF-α. The signaling pathways of VEGF, TNF-α, and IL-1β in endothelial cells have not yet been fully delineated (28), and further studies are necessary to address the relationships of these pathways and Id.

When HUVECs were treated with VEGF or TGFβ, expression of Id was induced. Expression of Id3 has been shown to be induced by the Ras-ERK pathway in thymocytes (17), and through type I receptor of the TGFβ via Smad1/5 signaling in HUVECs (18), whereas Id1 expression was associated with Raf/MEK1/2 activation in a human prostatic cancer cell line (29) and Smad1/5 signaling in HUVECs (18). Induction of Id in HUVECs by VEGF is reasonable, because MAPK cascade exists in the downstream of VEGF signaling pathways (30). In contrast, stimulation with IL-1β, TNF-α, or bFGF did not induce Id1 or Id3 in HUVECs, suggesting that Id may not be a ubiquitous mediator of inflammation, but more specifically associated with signaling pathways leading to angiogenesis.

For the knockdown experiments, we used double knockdown of Id1 and Id3, because knockdown of either one of them resulted in only partial inhibition of VEGF-induced activation or angiogenesis. Such results were expected, because it has been demonstrated that Id1 and Id3 have similar promoter region sequences, and exert overlapping biochemical functions; thus either one might be able to compensate the other, at least partially. In contrast, our results indicated that knockdown of both Id1 and Id3 was sufficient to abolish most of the angiogenic processes induced by VEGF in HUVECs, and Id2 and Id4 cannot compensate for the lack of Id1 and Id3. *ID1* and *ID3* shRNA sequences were designed from the 5′ region specific to each gene. Because RNAi can block gene expression only when the shRNA sequence is highly matched with the target gene (31), Id2 and Id4 expression were not considered to be suppressed.

Although Id3 overexpression up-regulated MMP9, knockdown of Id did not inhibit VEGF-induced up-regulation of MMP9. This suggests the presence of other pathways that lead to MMP9 up-regulation. Nevertheless, Id knockdown resulted in marked inhibition of tube formation in Matrigel. Such discrepancy may be explained by reduced expression of α_2 and β_1 integrins, whose

ligands are collagen and laminin, the main components of basement membranes and also of Matrigel (32, 33). Thus, Id seems to be involved in multiple pathways leading to activation of endothelial cells and angiogenesis. Although the functions of Id1 and Id3 are substantially overlapping (11, 14), it is intriguing to delineate the pathways from each Id protein to a multitude of endothelial cell activation and angiogenic processes. Indeed, our observations indicated some notable differences between the effects of Id1 and Id3 overexpression; for example, Id1 overexpression failed to up-regulate E-selectin and to protect HUVEC from apoptosis induced by serum starvation. It has recently been reported that Id1 down-regulates expression of thrombospondin-1, a suppressor of angiogenesis (34). It is also of interest to examine whether all of the angiogenic processes associated with Id can be explained by down-regulation of thrombospondin-1. To gain further insights, DNA microarray analysis is underway.

In conclusion, we demonstrated that Id plays an indispensable role for the VEGF-induced activation and angiogenic processes of HUVECs. Based on the inhibition of endothelial cell activation and angiogenesis with RNAi, as well as the low expression of Id in most of the normal adult tissues, Id should be considered an attractive target for the development of new therapeutic approaches for disorders associated with excessive angiogenesis.

References

1. Koch, A. E. 1998. Angiogenesis: implications for rheumatoid arthritis. *Arthritis Rheum. 41:951.*
2. Feldmann, M., F. M. Brennan, and R. N. Maini. 1996. Rheumatoid arthritis. *Cell 85:307.*
3. Firestein, G. S. 1996. Invasive fibroblast-like synoviocytes in rheumatoid arthritis: passive responders or transformed aggressors? *Arthritis Rheum. 39:1781.*
4. Sakurai, D., A. Yamaguchi, N. Tsuchiya, K. Yamamoto, and K. Tokunaga. 2001. Expression of *ID* family genes in the synovia from patients with rheumatoid arthritis. *Biochem. Biophys. Res. Commun. 284:436.*
5. Benezra, R., R. L. Davis, D. Lockshon, D. L. Turner, and H. Weintraub. 1990. The protein Id: a negative regulator of helix-loop-helix DNA binding proteins. *Cell 61:49.*
6. Lasorella, A., M. Noseda, M. Beyna, Y. Yokota, and A. Iavarone. 2002. Id2 is a retinoblastoma protein target and mediates signalling by Myc oncoproteins. *Nature 407:592.*
7. Wilson, R. B., M. Kiledjian, C. P. Shen, R. Benezra, P. Zwollo, S. M. Dymecki, S. V. Desiderio, and T. Kadesch. 1991. Repression of immunoglobulin enhancers by the helix-loop-helix protein Id: implications for B-lymphoid-cell development. *Mol. Cell. Biol. 11: 6185.*
8. Sun, X. H., N. G. Copeland, N. A. Jenkins, and D. Baltimore. 1991. Id proteins Id1 and Id2 selectively inhibit DNA binding by one class of helix-loop-helix proteins. *Mol. Cell. Biol. 11:5603.*
9. Hara, E., T. Yamaguchi, H. Nojima, T. Ide, J. Campisi, H. Okayama, and K. Oda. 1994. Id-related genes encoding helix-loop-helix proteins are required for G_1 progression and are repressed in senescent human fibroblasts. *J. Biol. Chem. 269:2139.*
10. Cooper, C. L., G. Brady, F. Bilia, N. N. Iscove, and P. J. Quesenberry. 1997. Expression of the Id family helix-loop-helix regulators during growth and development in the hematopoietic system. *Blood 89:3155.*
11. Norton, J. D., R. W. Deed, G. Craggs, and F. Sablitzky. 1998. Id helix-loop-helix proteins in cell growth and differentiation. *Trends Cell Biol. 8:58.*
12. Lasorella, A., T. Uo, and A. Iavarone. 2001. Id proteins at the cross-road of development and cancer. *Oncogene 20:8326.*
13. Rivera, R., and C. Murre. 2001. The regulation and function of the Id proteins in lymphocyte development. *Oncogene 20:8308.*
14. Yokota, Y. 2001. Id and development. *Oncogene 20:8290.*
15. Zebedee, Z., and E. Hara. 2001. Id proteins in cell cycle control and cellular senescence. *Oncogene 20:8317.*
16. Ohtani, N., Z. Zebedee, T. J. Huot, J. A. Stinson, M. Sugimoto, Y. Ohashi, A. D. Sharrocks, G. Peters, and E. Hara. 2001. Opposing effects of Ets and Id proteins on $p16^{INK4a}$ expression during cellular senescence. *Nature 409:1067.*
17. Bain, G., C. B. Cravatt, C. Loomans, J. Alberola-Ila, S. M. Hedrick, and C. Murre. 2001. Regulation of the helix-loop-helix proteins, E2A and Id3, by the Ras-ERK MAPK cascade. *Nat. Immunol. 2:165.*
18. Ota, T., M. Fujii, T. Sugizaki, M. Ishii, K. Miyazawa, H. Aburatani, and K. Miyazono. 2002. Targets of transcriptional regulation by two distinct type I receptors for transforming growth factor-β in human umbilical vein endothelial cells. *J. Cell. Physiol. 193:299.*
19. Lyden, D., A. Z. Young, D. Zagzag, W. Yan, W. Gerald, R. O'Reilly, B. L. Bader, R. O. Hynes, Y. Zhuang, K. Manova, and R. Benezra. 1999. Id1 and Id3 are required for neurogenesis, angiogenesis and vascularization of tumour xenografts. *Nature 401:670.*
20. Coppé, J.-P., A. P. Smith, and P.-Y. Desprez. 2003. Id proteins in epithelial cells. *Exp. Cell Res. 285:131.*
21. Jaffe, E. A., R. L. Nachman, C. G. Becker, and C. R. Minick. 1973. Culture of human endothelial cells derived from umbilical veins: identification by morphologic and immunologic criteria. *J. Clin. Invest. 52:2745.*
22. Yilmaz, A., S. Kliche, U. Mayr-Beyrle, G. Fellbrich, and J. Waltenberger. 2003. p38 MAPK inhibition is critically involved in VEGFR-2-mediated endothelial cell survival. *Biochem. Biophys. Res. Commun. 306:730.*
23. Lakka, S. S., C. S. Gondi, N. Yanamandra, W. C. Olivero, D. H. Dinh, M. Gujrati, and J. S. Rao. 2004. Inhibition of cathepsin B and MMP-9 gene expression in glioblastoma cell line via RNA interference reduces tumor cell invasion, tumor growth and angiogenesis. *Oncogene 23:4681.*
24. Sikder, H. A., M. K. Devlin, S. Dunlap, B. Ryu, and R. M. Alani. 2003. Id proteins in cell growth and tumorigenesis. *Cancer Cell 3:525.*
25. Ling, M.-T., X. Wang, X.-S. Ouyang, K. Xu, S.-W. Tsao, and Y.-C. Wong. 2003. Id-1 expression promotes cell survival through activation of NF-κB signaling pathway in prostate cancer cells. *Oncogene 22:4498.*
26. Lyden, D., K. Hattori, S. Dias, C. Costa, P. Blaikie, L. Butros, A. Chadburn, B. Heissig, W. Marks, L. Witte, et al. 2001. Impaired recruitment of bone-marrow-derived endothelial and hematopoietic precursor cells blocks tumor angiogenesis and growth. *Nat. Med. 7:1194.*
27. Kim, I., S.-O. Moon, S. H. Kim, H. J. Kim, Y. S. Koh, and G. Y. Koh. 2001. Vascular endothelial growth factor expression of intercellular adhesion molecule 1 (ICAM-1), vascular cell adhesion molecule 1 (VCAM-1), and E-selectin through nuclear factor-κB activation in endothelial cells. *J. Biol. Chem. 276: 7614.*
28. Pober, J. S. 2002. Endothelial activation: intracellular signaling pathways. *Arthritis Res. 4(Suppl. 3):S109.*
29. Ling, M. T., X. Wang, X. S. Ouyang, T. K. Lee, T. Y. Fan, K. Xu, S. W. Tsao, and Y. C. Wong. 2002. Activation of MAPK signaling pathway is essential for Id-1 induced serum independent prostate cancer cell growth. *Oncogene 21:8498.*
30. Takahashi, T., H. Ueno, and M. Shibuya. 1999. VEGF activates protein kinase C-dependent, but Ras-independent Raf-MEK-MAP kinase pathway for DNA synthesis in primary endothelial cells. *Oncogene 18:2221.*
31. Elbashir, S. M., W. Lendeckel, and T. Tuschl. 2001. RNA interference is mediated by 21- and 22-nucleotide RNAs. *Genes Dev. 15:188.*
32. Dickeson, S. K., J. J. Walsh, and S. A. Santoro. 1998. Binding of the α_2 integrin I domain to extracellular matrix ligands: structural and mechanistic differences between collagen and laminin binding. *Cell Adhes. Commun. 5:273.*
33. Davis, G. E., and C. W. Camarillo. 1995. Regulation of endothelial cell morphogenesis by integrins, mechanical forces, and matrix guidance pathways. *Exp. Cell Res. 216:113.*
34. Volpert, O. V., R. Pili, H. A. Sikder, T. Nelius, T. Zaichuk, C. Morris, C. B. Shiflett, M. K. Devlin, K. Conant, and R. M. Alani. 2002. Id1 regulates angiogenesis through transcriptional repression of thrombospondin-1. *Cancer Cell 2:473.*

ELSEVIER

Cardiovascular Research 65 (2005) 356–365

Cardiovascular Research

www.elsevier.com/locate/cardiores

Effects of ACE inhibitor and AT_1 blocker on dystrophin-related proteins and calpain in failing heart

Masaya Takahashi[a], Kouichi Tanonaka[a], Hiroyuki Yoshida[a], Ryo Oikawa[a], Miki Koshimizu[a], Takuya Daicho[a], Teruhiko Toyo-oka[b], Satoshi Takeo[a,*]

[a]*Department of Pharmacology, Tokyo University of Pharmacy and Life Science, 1432-1 Horinouchi, Hachioji, Tokyo 192-0392, Japan*
[b]*Department of Organ Pathophysiology and Internal Medicine, Tokyo University Hospital, Tokyo, Japan*

Received 16 July 2004; received in revised form 22 September 2004; accepted 22 September 2004
Available online 26 October 2004
Time for primary review 26 days

Abstract

Objectives: Genetic depletion of dystrophin-related protein (DRP) complex causes cardiomyopathy in animals and humans. We found in a previous study that some types of DRP were degraded and that calpain content was increased in rats with non-genetically induced heart failure. The present study was aimed at examining the effects of an angiotensin-I-converting enzyme inhibitor (ACEI) trandolapril (Tra) or an angiotensin II type 1 receptor blocker (ARB) candesartan (Can), both of which are known to improve the pathophysiology of chronic heart failure (CHF) on degradation of DRP in failing hearts.
Methods: Coronary artery-ligated (CAL) and sham-operated rats (Sham rats) were treated orally with 3 mg/kg/day trandolapril (Tra) or 1 mg/kg/day candesartan (Can) from the 2nd to 8th week after surgery.
Results: Hemodynamic parameters of CAL rats at the 8th week after CAL (8w-CAL) indicated heart failure. α-Sarcoglycan (SG) and dystrophin in the surviving left ventricle (surviving LV) of 8w-CAL rats decreased, whereas β-, γ-, and δ-SGs remained unchanged. Calcium-activated neutral proteases μ-calpain and m-calpain increased in the surviving LV at the 8th week of postmyocardial infarction. Proteolytic activity in the presence of 5 mM Ca^{2+} markedly increased at the 2nd and 8th weeks, whereas 50 μM Ca^{2+} slightly but significantly increased proteolysis of casein. Tra or Can treatment improved the hemodynamic parameters, attenuated changes in α-SG and dystrophin, and reversed both calpain contents and activities of the failing heart back to sham levels.
Conclusion: These results suggest that attenuation in calpain-induced degradation of DRP complex is a possible mechanism for the Tra- or Can-mediated improvement of the pathogenesis of CHF following myocardial infarction.

Keywords: Experimental; Heart; Organ and subcellular; Pathophysiology; Candesartan; Dystrophin; Heart failure; Sarcoglycan; Trandolapril

This article is referred to in the Editorial by S. Baudet (pages 299–301) in this issue.

1. Introduction

Dystrophin-related protein (DRP) complex consisting of dystrophin, sarcoglycans (SGs), and dystroglycans [1] was suggested to play an important role in the structural stabilization of sarcolemmal integrity [1,2]. Inherent mutation or depletion of SG and/or dystrophin genes causes muscular dystrophy and dilated cardiomyopathy (DCM) in humans and hamsters [3,4]. Recent studies have shown that δ-sarcoglycan (δ-SG) gene transfection mediated by recombinant adeno-associated virus improved cardiac function, sarcolemmal stability, and survival of TO-2 hamsters [5], which mimic dilated cardiomyopathy of humans. Furthermore, it has been reported that degradation of DRP was induced in enterovirus-induced cardiomyopathy [6]. Although degradation of DRP complex occurs in genetically induced or virus-infection-induced cardiomyopathy, altera-

* Corresponding author. Tel.: +81 426 76 4583; fax: +81 426 76 5560.
E-mail address: takeos@ps.toyaku.ac.jp (S. Takeo).

0008-6363/$ - see front matter © 2004 European Society of Cardiology. Published by Elsevier B.V. All rights reserved.
doi:10.1016/j.cardiores.2004.09.022

tions in DRP in non-genetically induced cardiomyopathy or heart failure remain to be elucidated. In a previous study, we showed that α-SG and dystrophin decrease in the failing rat heart following coronary artery ligation (CAL) [7], indicating the genesis of degradation of DPR in non-genetically induced or non-virus-mediated heart failure. We observed that the above animals with coronary artery ligation (CAL) induced chronic heart failure (CHF) with low cardiac output [8–10] and that the pathophysiological alterations, including myocardial energy metabolism [11] and G protein signaling [12] were partially reversed by treatment with an angiotensin-I-converting enzyme inhibitor (ACEI) or an angiotensin II type 1 receptor blocker (ARB). The present study was undertaken to determine whether ACEI and ARB might exert protective effects on degradation of DRP in chronic heart failure following myocardial infarction.

In a previous study, we suggested that protein contents of a calcium-activated protease, calpain, were increased, and its proteolytic activity was also increased in the failing rat heart [7]. This protease is present in cardiac muscles and is suggested to play a role in the protein turnover [13]. Sandmann et al. reported an increase in calpain at transcription and translation levels in the surviving left ventricular muscle after myocardial infarction without data on alterations in DRP [14]. The findings suggest that calpain contributes to the degradation of DRP complex in the failing heart following acute myocardial infarction (AMI) through activation of calpain. To test this suggestion, we characterized profiles of calpains during the development of cardiac failure and examined the effects of ACEI and ARB on changes in calpain isoform contents and activities in the failing heart.

2. Methods

2.1. Animals

Male Wistar rats (SLC, Hamamatsu, Japan) weighing 210–240 g were used in the present study. The animals were conditioned according to *Guide for the Care and Use of Laboratory Animals* as published by the US National Institutes of Health (NIH Publication No.85-23, revised 1996). The protocol of this study was approved by the Committee of Animal Use and Welfare of Tokyo University of Pharmacy and Life Science.

2.2. Operation

Myocardial infarction of rats was produced by occlusion of the left ventricular coronary artery according to the method described previously [8]. The left coronary artery was ligated approximately 2 mm from its origin with a suture under artificial ventilation with air (CAL rat). In the present study, we selected the animals with two elimination criteria, presence of abnormal Q wave (greater than 0.3 mV) in ECG (lead I) and greater than 10 g increase in body weight at the 2nd week after CAL. [9]. Approximately 65% of the CAL rats were employed in the present study. By these criteria, CAL rats with approximately 40% infarct area in the left ventricle were consistently produced. Sham-operated rats (Sham rats) were treated in a similar manner except for CAL.

2.3. Treatment with agents

Oral treatment of the CAL rats with 3 mg/kg/day of trandolapril (Tra; Aventis Pharma Japan, Tokyo, Japan) or 1 mg/kg/day of candesartan (Can; Takeda Chem. Indust., Osaka, Japan) once per day was performed from the 2nd to 8th week after the operation. Trandolapril or candesartan was suspended in 0.25% carboxymethylcellulose sodium for the oral administration. In a preliminary study, effects of various doses of trandolapril and candesartan ranging from 0.3 to 10 mg/kg/day and from 0.1 to 3 mg/kg/day, respectively, on degradation of DRP in CAL rats were examined. We found that the doses of 3 mg/kg/day for trandolapril and 1 mg/kg/day for candesartan were most effective in attenuation in the degradation of DRP of the CAL rat at the 8th week. Treatment with drugs from an earlier time after CAL increased the mortality of CAL animals. The doses of these agents employed were similar to those for the effects on hemodynamic parameters in previous studies by others and ourselves [11,15].

2.4. Hemodynamic parameters

Two and eight weeks after the operation, CAL (2w- and 8w-CAL) and Sham (2w- and 8w-Sham) rats were anesthetized with a gas mixture of nitrous oxide/oxygen (3:1) and 0.5–2.5% enflurane at a flow rate of 600 mL/min through a mask loosely placed over the nose (n=15 each) [9]. The pO_2, pCO_2, and pH of the blood were 95–110, 35–41, and 7.37–7.41 mm Hg, respectively. The left ventricular systolic pressure (LVSP), left ventricular end-diastolic pressure (LVEDP), right ventricular systolic pressure (RVSP), right ventricular end-diastolic pressure (RVEDP), mean arterial pressure (MAP), and heart rate (HR) were measured as described previously [7].

2.5. Determination of infarct size and isolation of membrane and cytosolic fractions

After determination of hemodynamic parameters of 15 rats, four CAL or Sham rats at the 2nd or 8th weeks after the operation were used for determination of their infarct sizes by the planimetric method described previously [8]. The hearts of 11 other rats in each group were quickly isolated. The isolated hearts were divided into the infarct area and the surviving left ventricular (surviving LV) free wall, and then their tissue weights were measured. Myocardial membrane and the cytosolic

fraction of six of 11 CAL or Sham rats were prepared from the surviving LV according to a modification of McMahon's method [16]. The membrane fraction was used for Western blot analysis of DRP proteins, whereas the cytosolic fraction was used for determination of calpains and calpastatin proteins. The hearts of five other rats in each group were for RT–PCR to determine mRNA expression of DRP complex. In another set of experiments, four drug-untreated or drug-treated 8w-CAL rats were used for determination of proteolytic activity of the surviving LV. Hemodynamic profiles of the rats used for proteolytic activity were similar to those in the corresponding CAL or Sham rats as above (data not shown). Throughout the text, "control" refers to unoperated drug-untreated rats.

2.6. RNA extraction and RT–PCR

Total RNA from surviving LV of 2w- or 8w-Sham and CAL rats treated with or without agents was extracted by using Isogen^{R} (Nippon Gene, Kyoto, Japan). Integrity of the extracted RNA was confirmed by agarose gel electrophoresis. The concentration of the RNA was determined by the optical absorption at 260 nm. For the isolation of cDNAs for DRP, first strand cDNAs were synthesized from total RNAs. Then, the cDNAs were amplified by RT–PCR using following primers: for α-SG: sense ACTCACAGGGCTGGCTAGGCTGGAACA (nucleotide position −30 to −4) and antisense CGTCTGTCTGGTGCCGGAGGTGAAGAA (1132 to 1158); for β-SG: sense CAGGCTGCACCGGACCAAG (−19 to −1) and antisense AAGGTCAAGCTGAGATCGGATC (1017 to 1040); for γ-SG: sense TCGTCAGGAATCAGTTCCTCAGTG (−46 to −23) and antisense ACATGAAGGCTGAGGCACAGCTC (913 to 937); for δ-SG: sense CCATGACCACTGGATTCTCAAGG (149 to 172) and antisense GATGGCTTCCATATTGCCAGCTTC (657-634); for dystrophin: sense AACAACTGAACAGCCGGTGGACAG (2423 to 2446) and antisense TGACTGCTGGATCCACGTCCTGAT (2880 to 2857); for GAPDH: sense GAATTCCATTGACCTCAACTACATGG (568 to 593) and antisense TTGCTGCAGTCTTACTCCTTGGAGGCCAT (961 to 989). These sequences were referred to the literatures by others [14,17,18].

2.7. Western blotting and detection of proteins

Western blotting analysis of SGs, dystrophin, calpains, and calpastatin was performed according to the method described previously but with some modifications [9]. For determination of SGs and dystrophin, membrane proteins were electrophoresed through a 10% or 4% SDS-polyacrylamide gel, respectively. The cytosolic fractions were also applied on a 10% SDS-polyacrylamide gel. For the Western blot, the proteins were transferred to polyvinylidene difluoride (PVDF) membranes (Immobilon, Millipore, Bedford, MA). The membranes and cytosolic fractions were then incubated with the following antibodies: 1:1500 diluted antibody of α-SC (NCL-a-SARC, Novocastra Laboratories, Newcastle, UK), 1:2000 diluted antibody of anti-β-SC (NCL-b-SARC, Novocatra Laboratories), 1:3000 diluted antibody of γ-SC (NCL-g-SARC, Novocastra Laboratories), 1:4000 diluted antibody of δ-SC, and 1:3000 diluted antibody of dystrophin (NCL-DYS1, Novocastra Laboratories) in phosphate-buffered saline (PBS) containing 10% Block Ace (Dainippon Pharmaceuticals, Osaka, Japan) and 0.1% Tween 20 and with 1:3000 diluted antibody of calpain (SA-255, BIOMOL, Plymouth Meeting, PA) and 1:1000 diluted antibody of calpastatin (MAB3084, Chemicon, Temecula, CA) in Tris-buffered saline containing 5% skim milk and 0.1% Tween 20. Detection and quantification of these proteins on the PVDF membrane were performed by the method described previously [9].

2.8. Ex vivo proteolytic activity in cytosolic fraction

In another set of experiments, casein proteolysis activity of the cytosolic fraction, where calpain was present, prepared from the surviving LV of the heart from the 8w-CAL rat treated with or without drugs was estimated ex vivo (n=4 each). The method for preparation of the cytosolic fraction of the surviving LV was described previously [7]. The cytosolic fraction in the presence or absence of 100 μM leupeptin (Sigma, St. Louise, MO), a relatively selective inhibitor of calpain, was incubated for 30 min in the buffer of the following composition: 0.4% (w/v) casein, 5 mM cysteine, and 100 mM imidazole/HCl (pH 7.5). $CaCl_2$ was added into the incubation medium at the final concentration of 50 μM for an estimation of μ-calpain activity or 5 mM for m-calpain activity [19,20]. The absorbance of the supernatant in the reaction mixture at 280 nm, which represents the absorbance for small peptide fragments with aromatic amino acids produced by calpain proteolysis, was measured using a spectrophotometer (U-Best 30, JASCO, Hachioji, Japan) [13].

2.9. Statistics

The results were expressed as means±S.E.M. All data were normally distributed. Statistical significance of differences in hemodynamics and SGs, dystrophin, calpain, and calpastatin contents was estimated using two-way analysis of variance (ANOVA) followed by Fisher's PLSD correction for multiple pairwise comparisons. Statistical significance of differences in casein proteolysis activity between Sham and CAL groups was estimated using two-way ANOVA. The relationship between two parameters was calculated by the least squares method. Differences with a probability of 5% or less were considered to be significant (p<0.05).

3. Results

3.1. Heart and lung weights

Body, heart, and lung weights of the rats at the 2nd and 8th weeks are shown in Table 1. Body weight at the 8th week after the operation was significantly decreased in trandolapril- or candesartan-treated Sham rats, whereas the body weights of CAL rats did not differ from those of trandolapril- or candesartan-treated CAL rats. The left ventricular (LV) weight/body weight ratio of the 2w-CAL rats did not significantly differ from that of the 8w-CAL rats. There were no significant differences in the left ventricular weight/body weight ratio between the 2w-CAL and 2w-Sham rat or between the 8w-CAL and 8w-Sham rats. In contrast, the right ventricular weight/body weight ratio increased in both 2w- and 8w-CAL rats as compared with the corresponding Sham rats. Long-term treatment with trandolapril or candesartan significantly attenuated the increases in LV and RV weight/body weight ratios of the 8w-CAL rats. Lung weight and the ratio of lung weight/body weight of the 2w- and 8w-CAL rats were significantly increased compared with those of the corresponding Sham group. Drug treatment significantly attenuated the increase in the lung weight/body weight ratio of the 8w-CAL rats.

In another set of experiments, the infarct areas of the 2w- and 8w-CAL rats covered approximately 40% of the left ventricle. Treatment with these drugs did not affect infarct size of CAL rats (Table 1). There was no infarction in the myocardium of the Sham rats.

3.2. Hemodynamic parameters

Hemodynamic indices of the CAL and Sham rats were measured at the 2nd and 8th weeks after the operation (Table 2). As compared to the Sham rat, the MAP and LVSP of the 2w- and 8w-CAL rats decreased, whereas HR did not change throughout the experiment. In contrast, the LVEDP of the 2w-CAL rats was increased 12-fold the Sham value and then further enhanced at the 8th week after CAL (20-fold the Sham value). There were no changes in these hemodynamic parameters of the Sham rats throughout the experiment.

Treatment of CAL rats with trandolapril or candesartan during the 2nd to 8th week after the operation attenuated the increase in LVEDP. Treatment of CAL and Sham rats with trandolapril or candesartan showed decreased MAP and LVSP compared with either the drug-untreated CAL rats or the corresponding Sham animals.

3.3. Myocardial dystrophin-related proteins

Fig. 1 shows the changes in myocardial DRP contents of the 2w- and 8w-CAL rats treated with and without trandolapril or candesartan, respectively. At the 2nd week after CAL, all SGs in the surviving LV did not change significantly compared to the Sham rat. At the 8th week after CAL, α-SG and dystrophin in the surviving LV decreased to approximately 60% and 75% of the corresponding Sham value, respectively. Treatment of CAL rats with trandolapril or candesartan restored the decrease in α-SG and dystrophin in the surviving LV. β-, γ-, and δ-SGs in the surviving LV of the CAL rat did not change throughout the experiment regardless of treatment or not with drugs.

The myocardial DRP contents in the Sham rat were similar to those of the control throughout the experiment regardless of treatment or not with drugs.

3.4. Relationship between a decrease in α-SG or dystrophin and an increase in LVEDP

LVEDP of the 8w-CAL rats treated without and with drugs was plotted against α-SG or dystrophin content of the surviving left ventricular muscle (Fig. 2). The LVEDP was inversely and highly related to α-SG content at the 8th week after CAL (left panel in Fig. 2). The LVEDP was also inversely related to dystrophin content (right panel in Fig. 2).

3.5. Myocardial calpains and calpastatin

Fig. 3 shows the changes in the myocardial μ- and m-calpains and calpastatin contents of the 2w- and 8w-CAL rats treated with and without trandolapril or candesartan. Both μ- and m-calpain contents in the surviving LV of the 2w-CAL rats increased to approximately 170% and 165% of the control, respectively. The m-calpain level in the 8w-CAL rats also increased similar to that of the 2w-CAL rat, whereas the μ-calpain content significantly but slightly increased (approximately 130% of the control). Treatment of the CAL rats with trandolapril or candesartan attenuated the increase in the m-calpain level in the surviving LV. Myocardial μ-calpain level in the surviving LV of the 8w-CAL rat treated with drugs was similar to that of the 8w-Sham rat. There were no changes in the myocardial μ- and m-calpain contents in the Sham rats treated with and without trandolapril or candesartan throughout the experiment.

The calpastatin content of the surviving LV in the 2w- and 8w-CAL rats did not change significantly. Treatment of the CAL rats with trandolapril or candesartan tended to increase calpastatin content. There were no significant changes in the myocardial calpastatin content in the Sham rats throughout the experiment regardless of treatment or not with drugs.

3.6. Calpain-like proteolytic activity of the cytosolic fraction

Differences in leupeptin-sensitive proteolysis of the cytosolic fraction of the heart were examined (Fig. 4). Casein was incubated with the cytosolic fraction prepared from the surviving LV of the 2w- or 8w-CAL and Sham rats in the presence of either 50 μM (upper panels) or 5 mM $CaCl_2$ (lower panels). Left panels in Fig. 3 show the time

Table 1
Body, heart, and lung weights of CAL and Sham rats treated with and without (Un) either trandolapril (Tra) or candesartan (Can)

	Body weight (g)	LV weight (g)	LV/body (mg/g)	RV weight (g)	RV/body (mg/g)	Lung weight (g)	Lung/body (mg/g)	Infarct size (% of total LV)
2nd week								
Sham	259±6	0.51±0.02	1.97±0.06	0.14±0.01	0.54±0.03	0.89±0.04	3.43±0.11	N.D.
CAL	228±8*	0.51±0.02	2.24±0.09	0.24±0.01*	1.05±0.06*	2.26±0.09*	9.91±0.51*	42±2
8th week								
Sham								
Un	324±8	0.60±0.05	1.87±0.06	0.16±0.01	0.49±0.01	1.07±0.04	3.30±0.08	N.D.
Tra	293±5#	0.52±0.06	1.79±0.08	0.12±0.01	0.42±0.01	0.96±0.03	3.27±0.04	N.D.
Can	295±3#	0.53±0.05	1.81±0.06	0.12±0.01	0.41±0.01	0.93±0.03	3.15±0.04	N.D.
CAL								
Un	297±8*	0.61±0.05	2.06±0.06	0.32±0.01*	1.08±0.07*	2.95±0.11*	9.93±0.39*	42±1
Tra	275±9*	0.51±0.04	1.84±0.04#	0.20±0.01*,#	0.74±0.05*,#	1.81±0.11*,#	6.67±0.46*,#	42±1
Can	282±4*	0.54±0.04	1.92±0.02#	0.23±0.01*,#	0.82±0.06*,#	2.21±0.15*,#	7.86±0.56*,#	41±3
p values								
2w vs. 8w (CAL)	<0.001	0.294	0.088	0.015	0.242	0.028	0.651	–
CAL vs. Sham	0.007	0.817	0.069	0.008	0.005	0.006	0.006	–
Interaction	0.071	0.452	0.144	0.040	0.329	0.048	0.221	–
CAL vs. Sham	<0.001	0.353	0.004	<0.001	<0.001	<0.001	<0.001	–
Treatment	0.064	0.484	0.004	<0.001	<0.001	0.005	<0.001	–
Interaction	0.019	0.512	0.021	0.011	<0.001	0.009	<0.001	–

Each value except for infarct size represents the mean±S.E.M. of 11 experiments. Infarct size represents the mean±S.E.M. of four experiments. *p* values represent statistical significance among CAL and Sham groups of the 2nd and 8th weeks or among drug-untreated and Tra- and Can-treated groups at the 8th week after the operation.
Abbreviations: CAL, coronary artery ligation; Sham, sham operation; BW, body weight; LV, left ventricle including scar tissue; RV, right ventricle; N.D., not detectable.
* $p<0.05$ vs. corresponding sham-operated group.
# $p<0.05$ vs. corresponding drug-untreated group at the 8th week.

Table 2
Hemodynamic parameters of CAL and Sham rats treated with and without (Un) either trandolapril (Tra) or candesartan (Can)

	MAP (mm Hg)	HR (beats/min)	LVSP (mm Hg)	LVEDP (mm Hg)	RVSP (mm Hg)	RVEDP (mm Hg)
2nd week						
Sham	119±2	406±2	152±4	1.9±0.5	29±2	0.7±0.1
CAL	114±2*	397±1	141±4*	22.1±1.1*	67±6*	1.2±0.3
8th week						
Sham						
Un	122±2	403±1	155±3	1.6±0.3	24±1	1.0±0.2
Tra	96±1#	401±1	128±3#	1.2±0.3	28±1	0.9±0.2
Can	105±3#	400±1	143±3#	1.0±0.2	26±1	0.9±0.1
CAL						
Un	110±3*	401±2	142±3*	32.1±0.6*	68±6*	1.3±0.2
Tra	92±1*,#	399±2	117±2*,#	17.5±0.7*,#	44±3*,#	0.8±0.1
Can	97±2*,#	399±1	124±2*,#	20.8±1.8*,#	46±4*,#	1.1±0.2
p values						
2w vs. 8w (CAL)	0.469	0.574	0.379	<0.001	0.494	0.672
CAL vs. Sham	0.022	0.663	0.021	<0.001	<0.001	0.883
Interaction	0.218	0.793	0.337	<0.001	0.324	0.781
CAL vs. Sham	0.064	0.151	0.020	<0.001	<0.001	0.614
Treatment	<0.001	0.784	0.004	<0.001	<0.001	0.834
Interaction	0.871	0.193	0.525	<0.001	<0.001	0.743

Each value represents the mean±S.E.M. of 15 experiments. *p* values represent statistical significance among CAL- and Sham-groups of the 2nd and 8th weeks or among drug-untreated and Tra- and Can-treated groups at the 8th week after the operation.
Abbreviations: CAL, coronary artery ligation; Sham, sham operation; MAP, mean arterial pressure; HR, heart rate; LVSP, left ventricular systolic pressure; LVEDP, left ventricular end-diastolic pressure; RVSP, right ventricular systolic pressure; RVEDP, right ventricular end-diastolic pressure.
* $p<0.05$ vs. corresponding sham-operated group.
# $p<0.05$ vs. corresponding drug-untreated group at the 8th week.

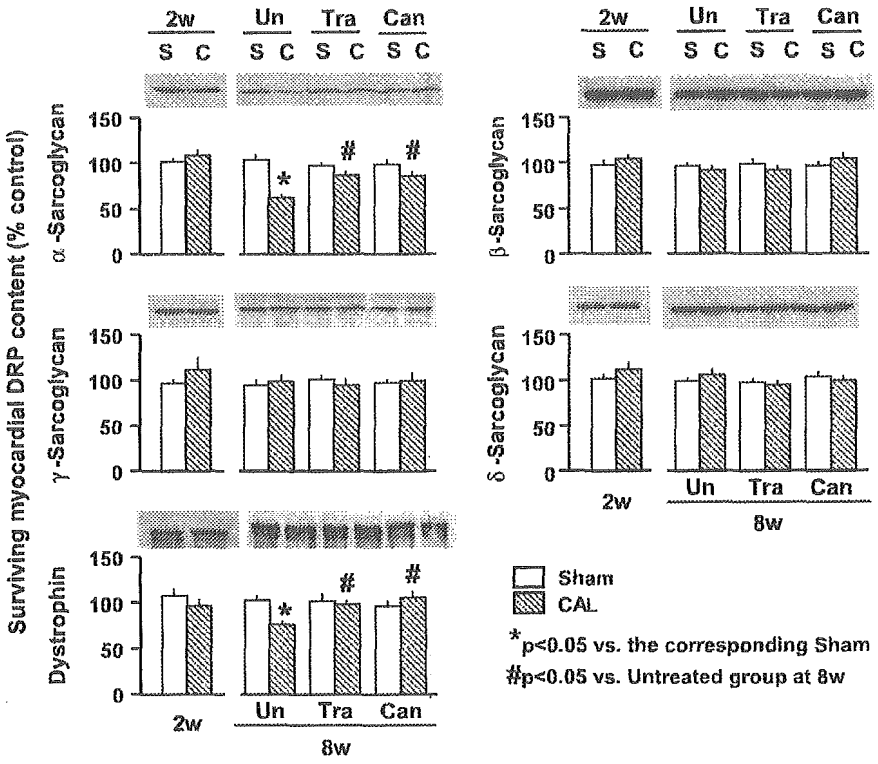

Fig. 1. Myocardial dystrophin-related proteins such as α-, β-, γ-, δ-sarcoglycans and dystrophin contents and the effects of trandolapril (Tra) and candesartan (Can) on these protein contents in the surviving left ventricular tissue of Sham and CAL rats 2 or 8 weeks after operation. Representative Western blots indicate 50-kDa bands for α-sarcoglycan, 43-kDa for β-sarcoglycan, 35-kDa for γ-Sarcoglycan, 35-kDa for δ-sarcoglycan, and 427-kDa for dystrophin in the surviving left ventricle. "Un" indicates animals without drug treatment. Each value represents the mean±S.E.M. of six experiments. *p<0.05 vs. corresponding sham-operated group. #p<0.05 vs. corresponding drug-untreated group at the 8th week. Statistical analysis was performed by two-way ANOVA followed by Fisher's multiple comparison as a post hoc test.

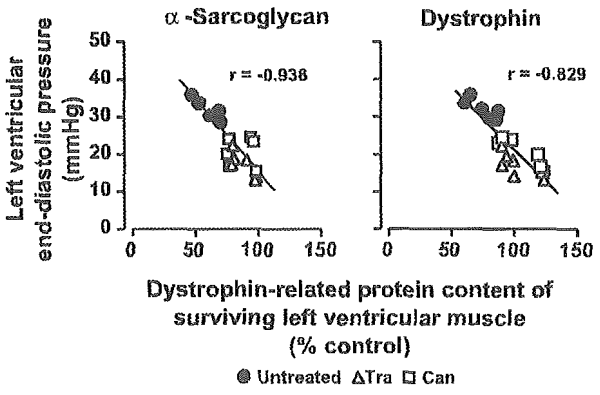

Fig. 2. Relationships between α-sarcoglycan (left panel) or dystrophin content (right panel) in the surviving left ventricular muscle and left ventricular end-diastolic pressure of the rat treated without (●) and with trandolapril (△) or candesartan (□) at the 8th week after coronary artery ligation. A significant relationship between α-sarcoglycan content in the surviving left ventricular muscle and left ventricular end-diastolic pressure (LVEDP) was observed (n=18; p<0.05). There was also a significant relationship between dystrophin content and LVEDP (n=18; p<0.05). The relationship between two parameters was calculated by the least squares method.

course of changes in the absorbance at 280 nm of the supernatant fluid of the incubation medium in the 2w-Sham and CAL rats, and the right panels show those in the 8w-Sham and CAL rats. In the presence of 50 μM $CaCl_2$, the absorbance reached submaximal level at 30-min incubation (left panels in Fig 4). Sixty-min incubation was required to reach at the submaximal level of the absorbance in the presence of 5 mM $CaCl_2$ (right panels in Fig 4). In the presence of low Ca^{2+} concentration, the casein proteolysis activity of the 2w-CAL rat was greater than that of the 8w-CAL rat. Casein proteolysis of the cytosolic fraction prepared from the 2w-CAL rat at the high concentration of Ca^{2+} was similar to that from 8w-CAL rat. The degree of the increase in the absorbance in the presence of 5 mM $CaCl_2$ was greater than that of 50 μM $CaCl_2$. As shown in Fig. 5, treatment of the CAL rats with trandolapril or candesartan attenuated the increase in casein proteolysis activity of the cytosolic fraction at both concentrations of Ca^{2+}.

3.7. Transcriptional changes in DRPs

Reverse transcription followed by PCR amplification of total RNA resulted in a single band of the predicted size for myocardial DRP or GAPDH. Fig. 6 shows the changes in

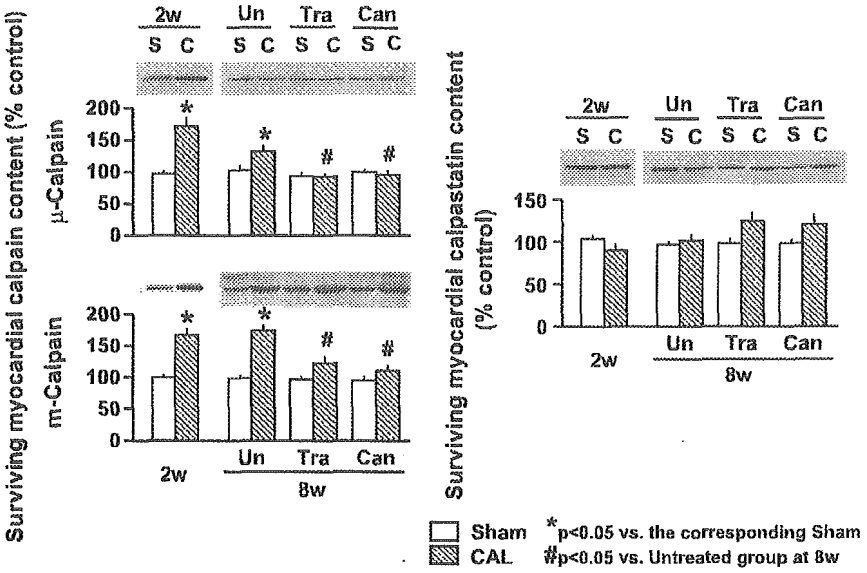

Fig. 3. Myocardial μ- (left upper) and m-CALpains (left lower) and calpastatin (right) contents and the effects of trandolapril (Tra) and candesartan (Can) on these protein contents in the surviving left ventricular tissue of Sham rats and CAL rats 2 or 8 weeks after the operation. Representative Western blots indicate 80-kDa bands for μ-calpain, 80-kDa for m-calpain, and 70-kDa for calpastatin in the surviving left ventricle. "Un" indicates animals without drug-treatment. Each value represents the mean±S.E.M. of six experiments. *$p<0.05$ vs. corresponding sham-operated group. #$p<0.05$ vs. corresponding drug-untreated group at the 8th week. Statistical analysis was performed by two-way ANOVA followed by Fisher's multiple comparison as a post hoc test.

mRNA levels of myocardial DRP of the 2w- and 8w-CAL rats treated with and without trandolapril or candesartan. mRNAs of α-SG, β-SG, and dystrophin in the surviving LV of the 2w-CAL rat increased (approximately 175%, 150%, and 160% of the control, respectively). α-SG and dystrophin

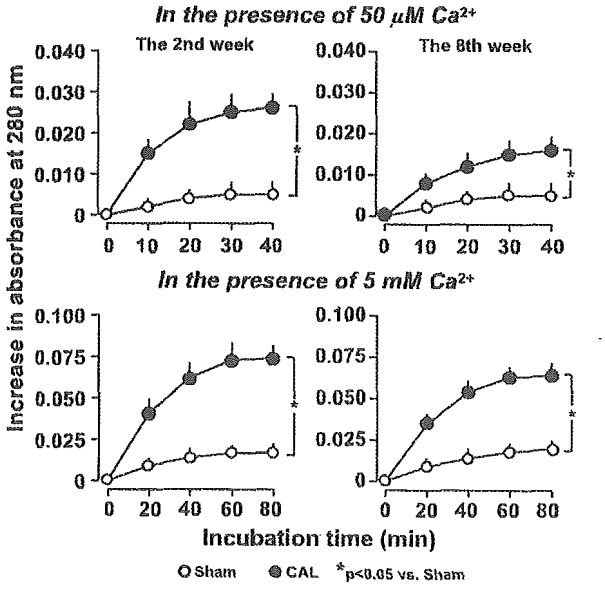

Fig. 4. The time course of changes in leupeptin-sensitive casein proteolysis activity of the myocardial cytosolic fraction of the surviving LV prepared from the Sham (○) and CAL rats (●) in the presence of 50 μM $CaCl_2$ (upper panels) and 5 mM $CaCl_2$ (lower panels) at the 2nd (left panels) and 8th weeks after the operation (right panels). Each value represents the mean±S.E.M. of four experiments. *$p<0.05$ vs. corresponding sham-operated group. Statistical analysis was performed by two-way ANOVA.

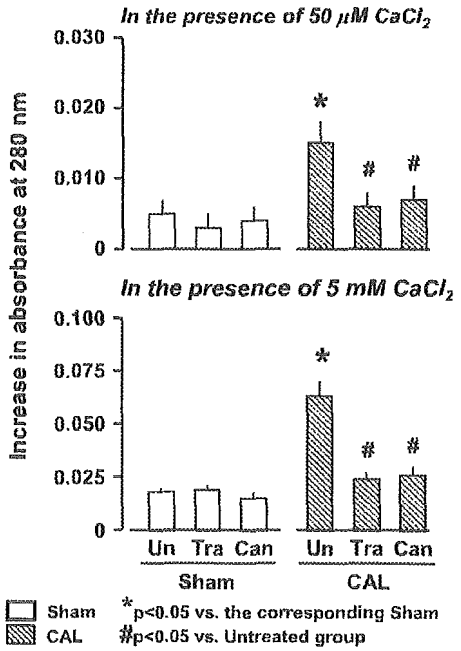

Fig. 5. Leupeptin-sensitive casein proteolysis activity of cytosolic fractions prepared from the 8w-Sham (open columns) and CAL rats (striped columns) without (Un) or with trandolapril (Tra) and candesartan (Can) treatment in the presence of 50 μM (the upper panel) and 5 mM $CaCl_2$ (the lower panel). Each value represents the mean±S.E.M. of four experiments. #$p<0.05$ vs. corresponding sham-operated group. *$p<0.05$ vs. corresponding drug-untreated group at the 8th week. Statistical analysis was performed by two-way ANOVA followed by Fisher's multiple comparison as a post hoc test.

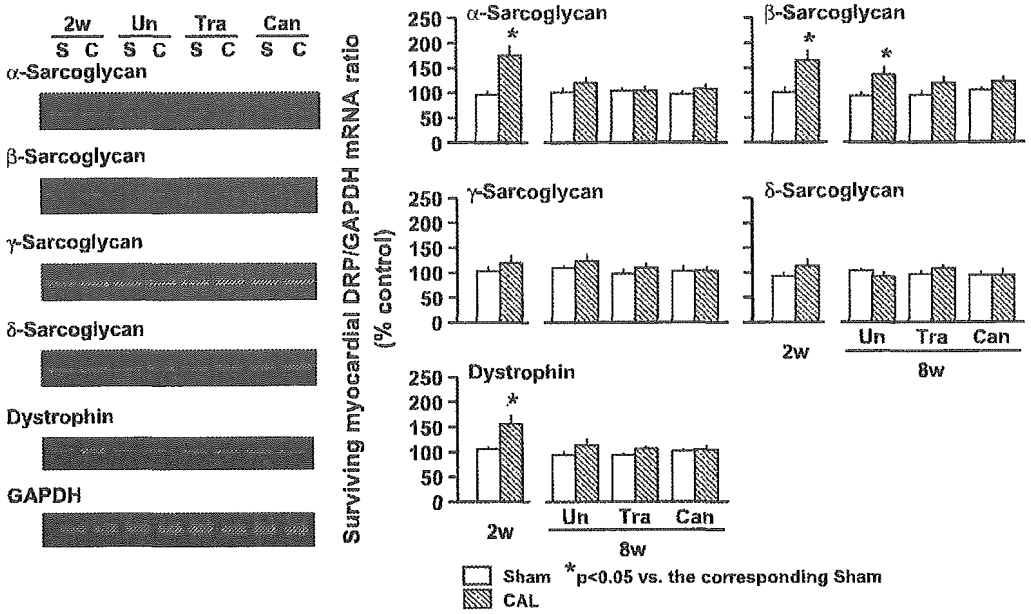

Fig. 6. Relative changes in mRNA expression of myocardial dystrophin-related proteins such as α-, β-, γ-, and δ-sarcoglycans and dystrophin levels and the effects of trandolapril (Tra) and candesartan (Can) on these mRNA levels in the surviving left ventricular tissue of Sham and CAL rats 2 or 8 weeks after operation. Left panels show representative PCRs that indicate for α-, β-, γ-, and δ-sarcoglycans for dystrophin and for GAPDH in the surviving left ventricle. "Un" indicates animals without drug-treatment. Each value represents the mean±S.E.M. of five experiments. *$p<0.05$ vs. corresponding sham-operated group. #$p<0.05$ vs. corresponding drug-untreated group at the 8th week. Statistical analysis was performed by two-way ANOVA followed by Fisher's multiple comparison as a post hoc test.

mRNA levels of the 8w-CAL rat were similar to those of the 8w-Sham rat, whereas β-SG mRNA levels were higher than that of the 8w-Sham rat (approximately 125% of the control). There were no significant changes in γ- and δ-SG mRNA levels in the surviving LV of the 2w- and 8w-CAL rats. Treatment with trandolapril or candesartan did not affect changes in α- and β-SGs and dystrophin mRNA in the surviving LV of the 8w-CAL rat. Drug treatment did not affect the expression of γ- and δ-SG mRNAs of the 8w-CAL rat. The myocardial mRNA levels of DRP complex in the 2w- and 8w-Sham rats were similar to those of the control rat regardless of treatment or not with drugs.

4. Discussion

Hemodynamic parameters of 8w-CAL rats suggested signs of heart failure in this model, which were consistent with those in our previous studies [7–12]. In this model, we also observed the left ventricular dysfunction with a decrease in cardiac output index at the 8th week after CAL, whereas cardiac function of the 2w-CAL rats was compensated [8,9]. Several clinical trials showed that ACEIs favorably affected the hemodynamics, improved the clinical symptoms [21,22], reduced the overall mortality, and ameliorated the left ventricular dysfunction in patients with congestive heart failure [22–24]. As for experimental studies, long-term treatment with trandolapril or candesartan resulted in a decrease in the body weight. The lower body weight of drug-treated animals is probably due to an increase in urine excretion, similar to the observation by others [25]. These drugs attenuated the elevation in LVEDP of the 8w-CAL rat, suggesting an improvement of the left ventricular function. These drugs attenuated the left and right ventricular hypertrophy and decreased the preload and afterload, as observed in previous [11,12,26] as well as present studies. Furthermore, it has been reported that ACEI and ARB attenuated an increase in collagen of the CAL animal [12]. These findings suggest that both drugs are capable of partially reversing cardiac remodeling.

We summarized the results on changes in DRP protein and calpain contents, mRNA levels, and proteolytic activity of the drug-untreated CAL and drug-treated CAL animals in Table 3. We found diverse changes in DRP complex in the failing heart, such as decreases in the α-SG and dystrophin contents in the surviving LV of the 8w-CAL rat, and no changes in β-, γ-, and δ-SGs throughout the experiment. The present findings showed that alterations in myocardial DRP complex occur in failing hearts following AMI in rats that have no genetic mutation of DRP complex and that have no viral infection. Myocardial dystrophin of the patients with ischemic cardiomyopathy decreased at the end stage [2]. Despite species differences between human and rat, our findings concerning a reduction in myocardial dystrophin were comparable to those of human ischemic cardiomyopathy [2]. Therefore, our experimental model appears to

Table 3
Summary of changes in dystrophin-related proteins, calpain, and calpastatin of the surviving LV after coronary artery ligation and effects of trandolapril and candesartan

	2nd week	8th week		
		Un	Tra	Can
Protein content				
α-Sarcoglycan	±	Decrease	Preserve	Preserve
β-Sarcoglycan	±	±	±	±
γ-Sarcoglycan	±	±	±	±
δ-Sarcoglycan	±	±	±	±
Dystrophin	±	Decrease	Preserve	Preserve
μ-Calpain	Increase	Increase	Reverse	Reverse
m-Calpain	Increase	Increase	Reverse	Reverse
Calpastatin	±	±	±	±
mRNA				
α-Sarcoglycan	Increase	±	±	±
β-Sarcoglycan	Increase	Increase	±	±
γ-Sarcoglycan	±	±	±	±
δ-Sarcoglycan	±	±	±	±
Dystrophin	Increase	±	±	±
Proteolytic activity				
Low Ca^{2+} (50 μM)	Increase	Increase	Reverse	Reverse
High Ca^{2+} (5 mM)	Increase	Increase	Reverse	Reverse

"±" in the table represents no change compared with the corresponding parameter of control animal.

mimic changes in DRP in the human myocardium with ischemic cardiomyopathy.

ACEI or ARB preserved the α-SG and dystrophin contents in the surviving LV, showing that α-SG and dystrophin were sensitive to contractile dysfunction of the rat heart among the DRPs and that the alteration in these proteins was associated timely with the development of heart failure following AMI and concertedly with the effects of the ACEI and ARB. Furthermore, there were significant and inverse relationships between α-SG or dystrophin contents and an increase in LVEDP, suggesting that decreases in these proteins may at least in part cause contractile dysfunction. These results suggest that alterations in α-SG and dystrophin may contribute to not only structural defects but also functional disorders of the failing hearts.

The mechanism underlying the decreases in α-SG and dystrophin after CAL should be addressed. We focused on μ- and m-calpains that were suggested to be activated in the ischemic heart [14] and found that these protease contents in the surviving LV of the 2w-CAL rat markedly increased. We also showed that the m-calpain level remained at a high level even after 8 weeks after CAL, whereas the μ-calpain level was slightly but significantly higher than that of the 8w-Sham rat. In contrast, myocardial calpastatin after CAL did not significantly alter throughout the experiment. Inasmuch as calpastatin has been shown to inhibit proteolytic activity of all calpain isoforms [27], the increase in calpain with no significant change in the calpstatin content in the CAL animal may lead to enhancement of the proteolytic activity. To examine the effect of these drugs on the proteolytic activity, the caseinolytic activity of the surviving LV of the CAL rat was determined. We found a marked increase in the casein proteolysis by the cytosolic fraction of the 8w-CAL animal in the presence of low and high concentrations of Ca^{2+}. The increased proteolysis was attenuated by leupeptin, a protease inhibitor with a relatively high affinity to calpain [13]. Thus, it is conceived that the former may represent the activity of μ-calpain and the latter that of m-calpain.

Furthermore, we found that mRNA expressions of α- and β-SGs and dystrophin were increased at the 2nd week after CAL. This implies that α- and β-SGs and dystrophin contents may be preserved at the 2nd week after CAL despite increases in proteolytic activity of calpains. In contrast, mRNA expressions of α-SG and dystrophin in the 8w-CAL rat were reversed to that in the 8w-Sham rat, whereas β-SG mRNA expression of the 8w-CAL rat was still higher than that of the corresponding Sham rat. Inasmuch as the μ- and m-calpain contents and proteolytic activity in the surviving LV of the 8w-CAL rat were greater than those of the corresponding Sham rat, digestion of DRP in the 8w-CAL rat may be enhanced, resulting in a reduction in α-SG and dystrophin contents. Recently, Toyo-oka et al. reported a significant relationship between cleavage of dystrophin and suppression of hemodynamic parameters of dilated cardiomyopathic hamster TO-2 [28]. They also showed that a decrease in myocardial dystrophin was observed in the isoprenaline-induced heart failure of rats and in the patient with dilated cardiomyopathy [28]. Thus, it appears that increased calpain proteolysis may provoke a decrease in myocardial dystrophin during the development of heart failure in animals and humans.

Trandolapril and candesartan attenuated the increase in μ- and m-calpain contents in the surviving LV of the 8w-CAL rat, whereas these drugs did not affect changes in mRNA levels of DRP. Trandolapril and candesartan attenuated the increase in the leupeptin-sensitive casein proteolysis of the 8w-CAL rat, suggesting that an increased level of calpain in the failing heart may contribute to degradation of DRP complex. Furthermore, these drugs tended to increase the calpastatin content in the surviving LV of the 8w-CAL rats. Thus, it is likely that these drugs are capable of suppressing the proteolytic activity of the CAL hearts, leading to attenuation of decreases in α-SG and dystrophin at the 8th week after AMI.

Alternatively, we have to consider the effect of the drugs on cardiac remodeling. That is, Tra and Can treatment elicited reduction in the systemic blood pressure during the development of heart failure and suppression of increases in the right and left ventricular weight/body weight after myocardial infarction. We cannot rule out the possibility that hemodynamic alterations and suppression of cardiac remodeling in Tra- and Can-treated CAL rats may play an important role in the prevention of the degradation of DRP. Further evidence is required to conclude such possibility.

References

[1] Ozawa E, Noguchi S, Mizuno Y, Hagiwara Y, Yoshida M. From dystrophinopathy to sarcoglycanopathy: evolution of a concept of muscular dystrophy. Muscle Nerve 1998;21:421–38.

[2] Vatta M, Stetson SJ, Prez-Verdia A, Entman ML, Noon GP, Torre-Aminoe G, et al. Molecular remodeling of dystrophin in patients with end-stage cardiomyopathies and reversal in patients on assistance-device therapy. Lancet 2002;359:936–41.

[3] Kunkel LM. Analysis of deletions in DNA from patients with Becker and Duchenne muscular dystrophy. Nature 1986;11:73–7.

[4] Melacini P, Fanin M, Duggan DJ, Freda MP, Berardinelli A, Danieli GA, et al. Heart involvement in muscular dystrophies due to sarcoglycan gene mutations. Muscle Nerve 1999;22:473–9.

[5] Kawada T, Nakazawa M, Nakauchi S, Yamazaki K, Shimamoto R, Urabe M, et al. Rescue of hereditary form of dilated cardiomyopathy by rAAV-mediated somatic gene therapy: amelioration of morphological findings, sarcolemmal permeability, cardiac performances, and the prognosis of TO-2 hamsters. Proc Natl Acad Sci U S A 2002; 99:901–6.

[6] Badorff C, Lee G-H, Lamphear BJ, Martone ME, Campbell KP, Rhoads RE, et al. Enteroviral protease 2A cleaves dystrophin: evidence of cytoskeletal disruption in an acquired cardiomyopathy. Nat Med 1999; 5:320–6.

[7] Yoshida H, Takahashi M, Koshimizu M, Tanonaka K, Oikawa R, Toyo-oka T, et al. Decrease in sarcoglycans and dystrophin in failing heart following acute myocardial infarction. Cardiovasc Res 2003;59:419–27.

[8] Sanbe A, Tanonaka K, Hanaoka Y, Katoh T, Takeo S. Regional energy metabolism of failing heart following myocardial infarction. J Mol Cell Cardiol 1993;25:995–1013.

[9] Yoshida H, Tanonaka K, Miyamoto Y, Abe T, Takahashi M, Anand-Srivastava MB, et al. Characterization of cardiac myocyte and tissue β-adrenergic signal transduction in rats with heart failure. Cardiovasc Res 2001;50:34–45.

[10] Tanonaka K, Furuhama K, Yoshida H, Kakuta K, Miyamoto Y, Takeo S. Protective effect of heat shock protein 72 on the contractile function of the perfused failing heart. Am J Physiol 2001;281:H215–22.

[11] Sanbe A, Tanonaka K, Kobayashi R, Takeo S. Effects of long-term therapy with ACE inhibitors, captopril, enalapril and trandolapril, on myocardial energy metabolism in rats with heart failure following myocardial infarction. J Mol Cell Cardiol 1995;27: 2209–22.

[12] Yoshida H, Takahashi M, Tanonaka K, Maki T, Nasa Y, Takeo S. Effects of ACE inhibition and angiotensin II type 1 receptor blockade on cardiac function and G proteins in rats with chronic heart failure. Br J Pharmacol 2001;134:150–60.

[13] Toyo-oka T, Shimizu T, Masaki T. Inhibition of proteolytic activity of calcium activated neutral protease by leupeptin and antipain. Biochem Biophys Res Commun 1978;82:484–91.

[14] Sandmann S, Yu M, Unger T. Transcriptional and translational regulation of calpain in the rat heart after myocardial infarction—effects of AT1 and AT2 receptor antagonists and ACE inhibitor. Br J Pharmacol 2001;132:767–77.

[15] Hanatani A, Yoshiyama M, Takeuchi K, Kim S, Nakayama K, Omura T, et al. Angiotensin II type 1-receptor antagonist candesartan cilexitil prevents left ventricular dysfunction in myocardial infracted rats. Jpn J Pharmacol 1998;78:45–54.

[16] McMahon KK. Developmental changes of the G proteins–muscarinic cholinergic receptor interactions in rat heart. J Pharmacol Exp Ther 1989;251:372–7.

[17] Hanada H, Yoshida T, Pan Y, Iwata Y, Nishimura M, Shigekawa M. mRNA expression and cDNA sequences of β- and γ-sarcoglycans are normal in cardiomyopathic hamster heart. Biol Pharm Bull 1997;20:134–7.

[18] Noguchi S, Wakabayashi E, Imamura M, Yoshida M, Ozawa E. Developmental expression of sarcoglycan gene products in cultured myocytes. Biochem Biophys Res Commun 1999;262:88–93.

[19] Kambayashi J-I, Sakon M. Calcium-dependent proteases and their inhibitors in human platelets. In: Hawiger J, editor. Platelets: Receptors, Adhesion, Secretion Methods in Enzymology, vol. 169. San Diego, CA: Academic Press, 1989. p. 442–54.

[20] Waxman L. Calcium-activated proteases in mammalian tissues. Lorand L, editor. Methods in Enzymology, vol. 80. New York, NY: Academic Press, 1981. p. 664–80.

[21] Pfeffer MA, Braunwald E, Moye LA, Basta L, Brown Jr EJ, Cuddy TE, et al. Effect of captopril on mortality and morbidity in patients with left ventricular dysfunction after myocardial infarction Results of the survival and ventricular enlargement trial The SAVE Investigators. N Engl J Med 1992;327:669–77.

[22] McKelvie RS, Yusuf S, Pericak D, Avezum A, Burns RJ, Probstfield J, et al. Comparison of candesartan, enalapril, and their combination in congestive heart failure: randomized evaluation of strategies for left ventricular dysfunction (RESOLVED) pilot study. The RESOLVD Pilot Study Investigators. Circulation 1997;100:1056–64.

[23] Kober L, Torp-Pedersen C, Carlsen JE, Bagger H, Eliasen P, Lyngborg K, et al. A clinical trial of the angiotensin-converting-enzyme inhibitor trandolapril in patients with left ventricular dysfunction after myocardial infarction. Trandolapril Cardiac Evaluation (TRACE) Study Group. N Engl J Med 1995;333:1670–6.

[24] Pitt B, Segal R, Martinez FA, Meurers G, Cowley A, Thomas I, et al. Randomised trial of losartan versus captopril in patients over 65 with heart failure (Evaluation of Losartan in the Elderly Study, ELITE). Lancet 1997;349:747–52.

[25] Kraly FS, Corneilson R. Angiotensin II mediates drinking elicited by eating in the rat. Am J Physiol 1990;258:R436–42.

[26] Böhm M, Zolk O, Flesch M, Schiffer F, Schnabel P, Stasch J-P, et al. Effects of angiotensin II type 1 receptor blockade and angiotensin-converting enzyme inhibition on cardiac β-adrenergic signal transduction. Hypertension 1998;31:747–54.

[27] Suzuki K, Imajoh S, Emori Y, Kawasaki H, Minami Y, Ohno S. Calcium activated neutral protease and its endogenous inhibitor: activation at the cell membrane and biological function. FEBS Lett 1987;220:271–7.

[28] Toyo-oka T, Kawada T, Nakata J, Xie H, Urabe M, Masui F, et al. Translocation and cleavage of myocardial dystrophin as a common pathway to advanced heart failure: a scheme for the progression of cardiac dysfunction. Proc Natl Acad Sci U S A 2004;101:7381–5.

Available online at www.sciencedirect.com
SCIENCE DIRECT
Biochimica et Biophysica Acta 1751 (2005) 73–81
BIOCHIMICA ET BIOPHYSICA ACTA
BBA
http://www.elsevier.com/locate/bba

Review

A novel scheme of dystrophin disruption for the progression of advanced heart failure

Tomie Kawada[a], Fujiko Masui[b], Asaki Tezuka[b], Takashi Ebisawa[b], Hiroyuki Kumagai[c], Mikio Nakazawa[d], Teruhiko Toyo-oka[b,c,*]

[a]*Division of Pharmacy, Niigata University of Medical and Dental Hospital, Niigata, 951-8520, Japan*
[b]*Department of Pathophysiology and Internal Medicine, University of Tokyo, Tokyo 113-0033, Japan*
[c]*Department of Molecular Cardiology, Tohoku University, Biomedical Engineering Research Organization (TUBERO), Sendai 980-8587, Japan*
[d]*Department of Medical Technology School of Health Science, Faculty of Medicine, Niigata University, Niigata 951-8510, Japan*

Received 21 May 2004; received in revised form 15 December 2004; accepted 7 January 2005
Available online 26 January 2005

Abstract

The precise mechanism of the progression of advanced heart failure is unknown. We assessed a new scheme in two heart failure models: (I) congenital dilated cardiomyopathy (DCM) in TO-2 strain hamsters lacking δ-sarcoglycan (SG) gene and (II) administration of a high-dose of isoproterenol, as an acute heart failure in normal rats. In TO-2 hamsters, we followed the time course of the histological, physiological and metabolic the progressions of heart failure to the end stage. Dystrophin localization detected by immunostaining age-dependently to the myoplasm and the in situ sarcolemma fragility evaluated by Evans blue entry was increased in the same cardiomyocytes. Western blotting revealed a limited cleavage of the dystrophin protein at the rod domain, strongly suggesting a contribution of endogenous protease(s). We found a remarkable up-regulation of the amount of calpain-1 and -2, and no change of their counterpart, calpastatin. After supplementing TO-2 hearts with the normal δ-SG gene in vivo, these pathological alterations and the animals' survival improved. Furthermore, dystrophin but not δ-SG was disrupted by a high dose of isoproterenol, translocated from the sarcolemma to the myoplasm and fragmented. These results of heart failure, irrespective of the hereditary or acquired origin, indicate a vicious cycle formed by the increased sarcolemma permeability, preferential activation of calpain over calpastatin, and translocation and cleavage of dystrophin would commonly lead to advanced heart failure.

Keywords: Dystrophin; δ-Sarcoglycan (SG); Gene therapy; Heart failure; Proteolysis; Calpain

1. Background

Advanced heart failure is the most prevalent cause of death or hospitalization in developed countries. Although several pharmacological agents have improved its mortality or morbidity of the patients [1–4], no treatment is available to completely prevent its progression, with the exception of cardiac transplantation. However, this therapy encompasses a variety of socioeconomic and medical limitations. Specifically, in infantile and juvenile cases, cardiac transplantation is accompanied with some problems such as mismatch in organ size. End-stage DCM is the most frequent cause of heart transplantation in Japan.

The precise mechanism remains unknown of the progression of advanced heart failure. Its clarification is urgently required for prevention or treatment. We conducted a comprehensive study of the progression of cardiac dysfunction in advanced heart failure, and propose our paradigm that the disruption of dystrophin or dystrophin-associated proteins (DAP) may aggravate heart failure. DAP forms a complex connecting dystrophin at the subsarco-

Abbreviations: CM, cardiomyopathy; DCM, dilated cardiomyopathy; δ-SG, δ-sarcoglycan; DAP, dystrophin-associated proteins; HCM, hypertrophic cardiomyopathy; LVP, left ventricular pressure; rAAV, recombinant adeno-associated virus

* Corresponding author. Tel.: +81 3 5841 2570; fax: +81 3 3813 2009.
E-mail address: toyooka_3im@hotmal.com (T. Toyo-oka).

1570-9639/$ - see front matter © 2005 Elsevier B.V. All rights reserved.
doi:10.1016/j.bbapap.2005.01.001

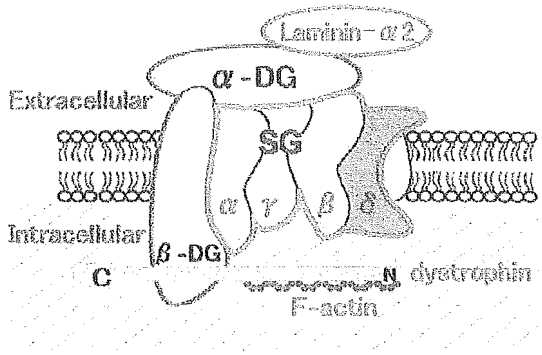

Fig. 1. A scheme of dystrophin-associated proteins (DAP). Mutations in DAP, which cause DCM in human cases, are shown in red characters. SG: sarcoglycan; DG: dystroglycan.

lemma with laminin α-2 at the extracellular matrix (Fig. 1). Cardiac muscle repeats contraction and relaxation throughout its life and the sarcolemma should be more resistant to the expansion–shrinkage cycling in cardiac than in skeletal muscle. The hereditary origin of DCM is estimated to account for about 20% to 30% of all patients [5,6]. A gene defect in DAP and subsequent dysfunction of the corresponding protein commonly induce DCM, as is the case in Duchenne or Becker type muscular dystrophy [7].

2. Merits of TO-2 strain hamsters for the study of DCM

Animal models are very significant for both the assessment of pathological processes and the development of new treatments [8]. The cardiomyopathy (CM) hamster is a valuable model of human hereditary CM [9] and shows hypertrophic CM in the BIO 14.6 strain [9–11] and DCM in the TO-2 strain of hamsters [11]. Many pathological and physiological features have been reported, including oncosis, apoptosis and necrosis of myocardial cells, interstitial fibrosis and calcification (Fig. 2). We showed that both HCM and DCM hamsters share a common defect in δ-SG gene, a component of DAP (Fig. 1, Refs. [11,12]), and determined the breakpoint of the δ-SG gene in both strains [11]. δ-SG makes a complex with other α-, β- and γ-SGs and connects dystrophin with the extracellular matrix via α- and β-dystroglycan [13–15]. In the BIO 14.6 myocardium at the early stages of heart failure, both the β- and δ-SG proteins were missing, but α- and γ-SG were weakly and heterogeneously expressed in cardiomyocytes. In contrast, the TO-2 strain shows loss of other SGs from the onset [16]. We conclude that TO-2 was suitable for developing gene therapy of the hereditary DCM.

Similar mutations of the δ-SG gene have been reported in patients of four families with DCM, one of who underwent cardiac transplantation [17]. Accordingly, the same δ-SG gene mutation causes DCM in both humans and hamsters. Most gene mutations in animals have been demonstrated in humans. This is the evidence that the genes of all animals have mutated to differentiate or adapt to changing environments. At present, mutations of cardiac F-actin, α-, β-, γ-, and δ-SG or lamin A/C have been reported to cause DCM in humans [7,17–21].

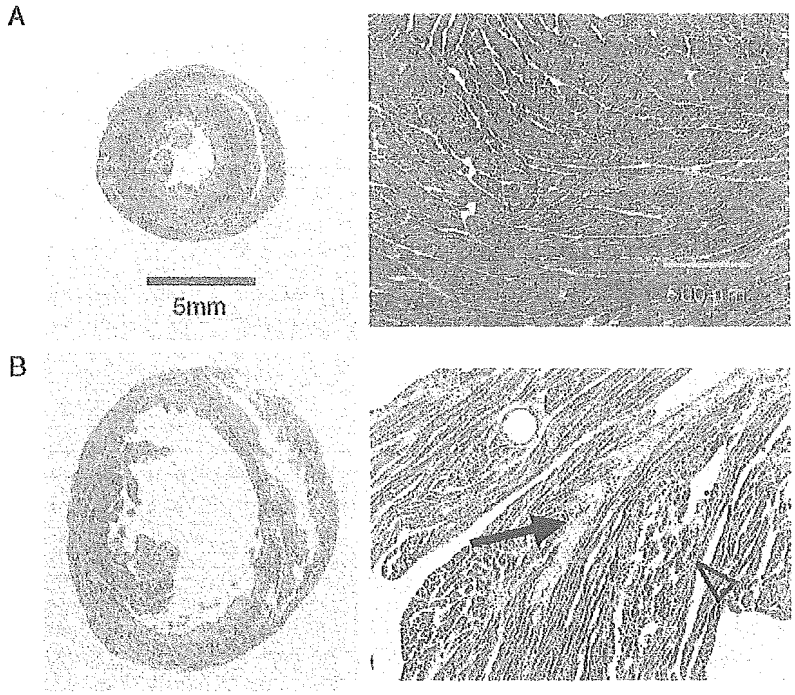

Fig. 2. Pathological features of normal (A, F1B) and DCM (B, TO-2) hamster hearts. TO-2 showed the enlarged cardiac chamber. The arrow and arrowhead denote interstitial fibrosis and calcified lesion, respectively.

Another benefit of TO-2 hamsters is that they are very useful for studying gene therapy. We have succeeded in the rescue of DCM in TO-2 hamsters, using recombinant adeno-associated virus (rAAV) vector-mediated gene transduction in vivo with normal δ-SG [22,23]. In these studies, we found that DAP may play an important role in the progression of advanced heart failure. Although hereditary DCM is caused by congenital loss of the δ-SG protein, the reasons for which the TO-2 strain does not show overt cardiac failure at birth and also shows a slow progression of clinical symptoms have not been clarified yet. Similarly, the late onset of the hereditary genetic diseases has been reported in Duchenne type muscular dystrophy [24] and Huntington's atoxia [25]. To verify our scheme that muscular dystrophy-like lesions in cardiac muscle may induce advanced heart failure, we followed the time course of hemodynamics, immunostaining and Western blotting of dystrophin and the in situ sarcolemma permeability by Evans blue uptake.

At the meeting of the International Protease Society at Nagoya, we demonstrated that myocardial dystrophin was age-dependently cleaved and translocated from the sarcolemma to the myoplasm. The amount of dystrophin was closely correlated with hemodynamic indices and animal's survival as described in our recent data [26].

We briefly present data on gene therapy using our hereditary model [22,23]. Then, we discuss the acquired acute heart failure model produced by the administration of high-dose of isoproterenol to rats [27].

3. Detailed evaluation of the DCM progression in the hereditary model with gene therapy

Gene therapy is promising for the treatment of hereditary DCM. Both the limited and transient expression after in vivo gene transfer precludes a functional evaluation of the transduced hearts [16,28]. We examined the long-term effect of the gene delivery using the rAAV vector. This vector is non-pathogenic [29,30] and has been approved for therapy of human patients with cystic fibrosis [31] and hemophilia B [32].

The rAAV vectors were constructed with a normal δ-SG gene or reporter (Lac Z) gene, both of which were driven by a CMV promoter. The detailed methods of gene therapy were described previously [22]. These vectors were intramurally administered to the apex and the left ventricular free wall of the TO-2 hamster by open-chest surgery at 5 weeks of age. Then, animals were cared for 35 weeks after transduction.

3.1. Northern and Western blotting analyses of δ-SG

To identify the transcription and in vivo expression of the SG complex, mRNA was purified from the hearts 10 weeks after transduction. Blot analysis of total mRNA detected two

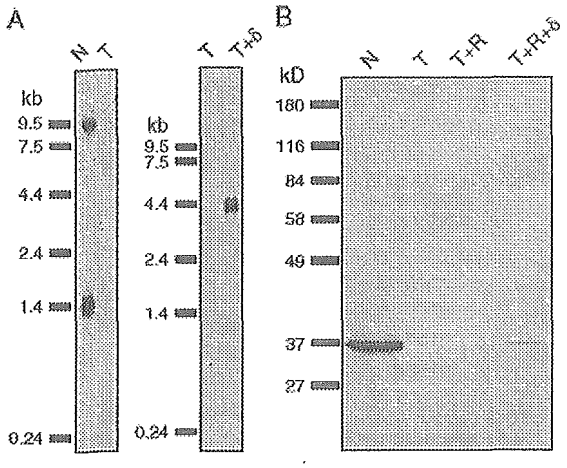

Fig. 3. Expressions of transcript (A) and transgene (B) of δ-sarcoglycan (SG) in hamster hearts. (A) Two micrograms poly (A)+RNA was applied per lane. N, normal strain; T, TO-2 strain without gene transduction; T+δ, TO-2 with transduction at 10 weeks after δ-SG gene transduce to 5-week-old hamsters by rAAV-mediated vector. (B) Fifty micrograms of total homogenate protein was applied per lane. Note that the in vivo gene transduce of reporter gene (Lac Z) alone demonstrated no band (T+R). However, when δ-SG gene was transduced in vivo together with Lac Z (T+R+δ), a thin but distinct band with the same mobility as the positive control hamster heart [21].

major δ-SG transcripts in the heart of normal hamsters (Fig.3A, N, Ref. [22]). Both bands were missing in untreated TO-2 hamsters (Fig. 3A, T), secondary to the gene deletion 6.7 kb upstream of exon 2 including the promoter and exon 1 [11]. In the hearts of transduced TO-2 hamsters, a single robust transcript was present (Fig. 3A, T+δ), suggesting that the rAAV-mediated transgene for δ-SG was expressed over a broad region in an appreciable amount.

Western blotting of heart samples of the normal hamsters showed a clear band (Fig. 3B, N, Ref. [22]). In contrast, the TO-2 strain had no band at all (Fig. 3B, T). The in vivo transfer of the reporter gene demonstrated no band 10 weeks after the transduction (Fig. 3B, T+R). However, when the δ-SG gene was transduced in vivo together with a reporter gene, a distinct band of the same molecular mass was demonstrated as a positive control (Fig. 3B, T+R+δ).

We employed serial sections using antibodies specific to each protein for immunostaining of the reporter (β-Gal) and δ-SG transgenes [23]. The long-lasting rAAV vector is very useful for the therapy of degenerative disease. Both the reporter and δ-SG transgenes were detected 35 weeks after (40 weeks of age) in the transduced TO-2 hearts, indicating that the transgene was expressed throughout the animal's life span [33]. The β-Gal expressing cells accounted for 40% of total cells in the apex, where the vector was injected [22].

β-Gal expression was exclusively shown in the cytoplasm of cardiomyocytes (Fig. 4A), indicating that β-Gal did not require translocation after biosynthesis. It should be noted that most myocardial cells presenting β-Gal matched those cells exhibiting δ-SG (Fig. 4B). The expression of δ-SG was not restricted to the sarcolemma as the cytoplasm in